The ancient steel sword and armour technology revealed through advanced neutron imaging techniques

Francesco Grazzi

Consiglio Nazionale delle Ricerche
Istituto Sistemi Complessi

Research group

Francesco Grazzi[1], Anna Fedrigo[1,2], Filomena Salvemini[3], Nikolay Kardjilov[4], Eberhard Lehmann[5], Steven Peetermans[5], Burkhard Schillinger[6], Takenao Shinohara[7], Yoshiaki Kiyanagi[8], Anton Tremsin[9], Francesco Civita[10], David Edge[11], Alan Williams[11]

1 Consiglio Nazionale delle Ricerche, Istituto dei Sistemi Complessi, Italy
2 Niels Bohr Institute, Kopenhagen University, Denmark, and European Spallation Source ESS AB, Sweden
3 Australian Nuclear Science and Technology Organization, Bragg Institute, Australia
4 Helmholtz Zentrum Berlin, BER-II, Germany
5 Paul Scherrer Institute, SINQ Neutron Source, Switzerland
6 Technische Universitaet Munchen, FRM-II, Germany
7 J-PARC Neutron Source, Japan
8 Nagoya University, Graduate School of Engineering
9 University of California at Berkeley, Space Sciences Laboratory, USA
10 Museo Stibbert, Italy
11 The Wallace Collection, UK

Outline

- Historical swords and their properties
- Metallurgy of steel
- What neutron imaging can do
- Samples and results
- A unique feature
- Conclusions

Historical armours and their properties

- purposedly created as protection mainly for sensitive parts: head and chest
- able to stop or slow down hits
- should protect against slashing, piercing and crushing
- Could be as hard as possible and/or able to change shape to absorb blows
- Made of natural hard materials or of steel and iron when enough metal became available

Characteristics:

- portable
- absorbing or deviating hits
- resilient body

Historical swords and their properties

- first tool purposedly created as weapon
- made by a handle and a long cutting body (one or two edges) and a sharp tip

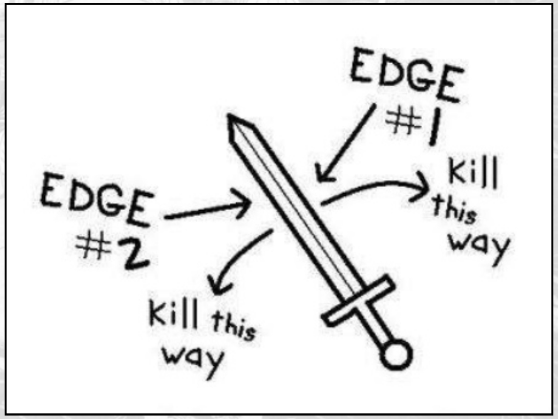

- used for slashing and piercing
- used with one or two hands

Characteristics:

- hard edge and tip
- resilient body

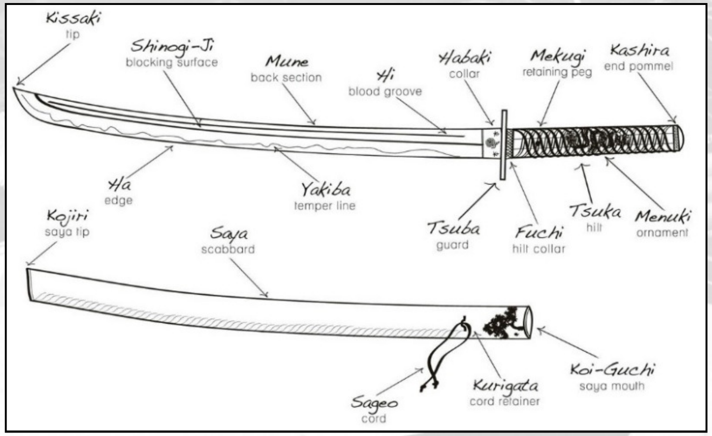

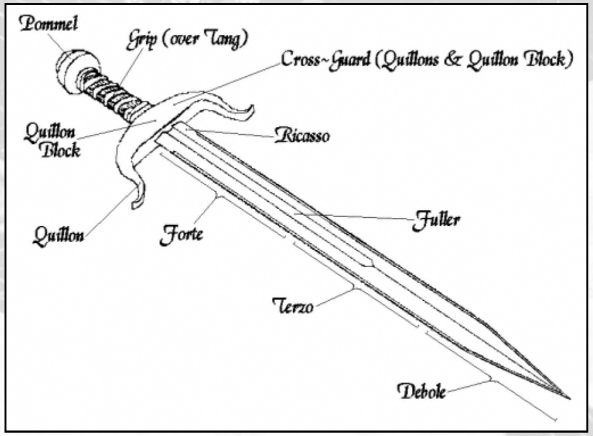

Metallurgy of steel

Quasi-equilibrium phase diagram of carbon steel

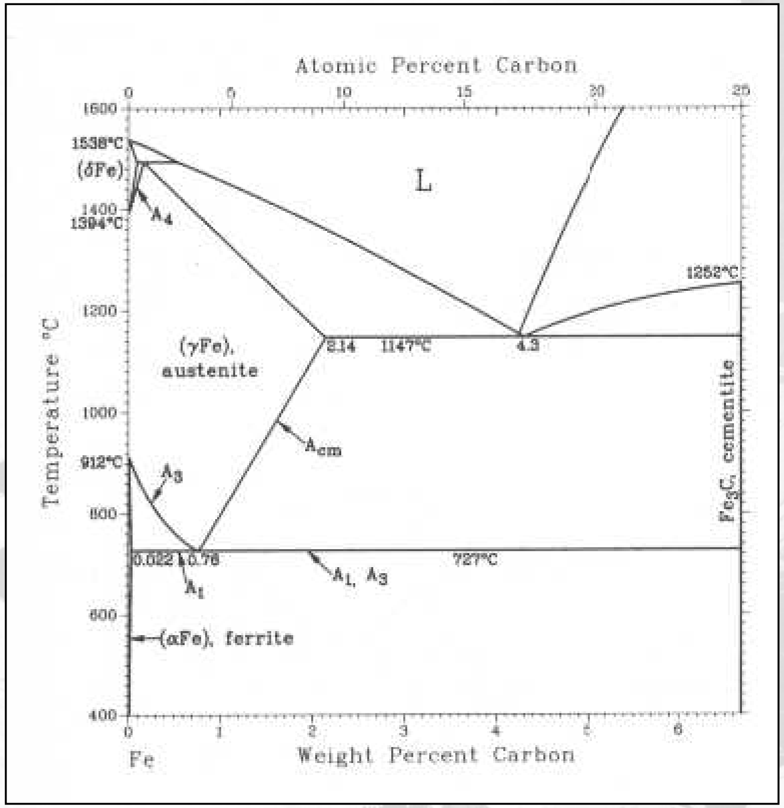

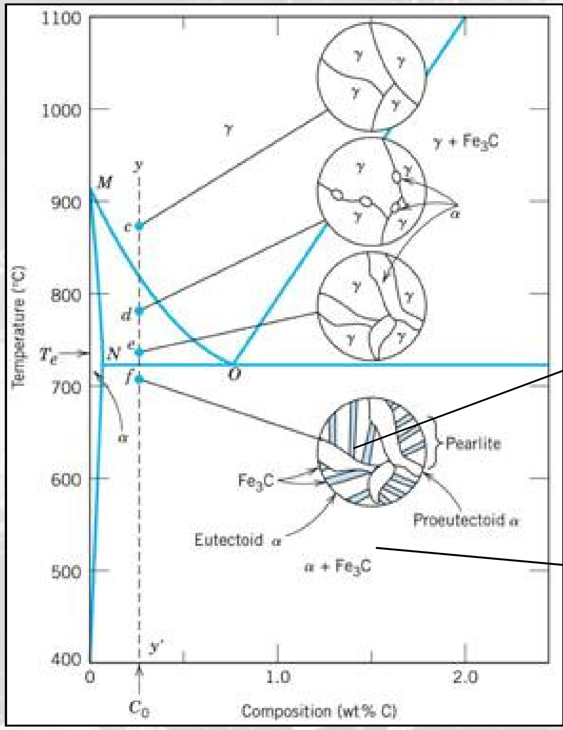

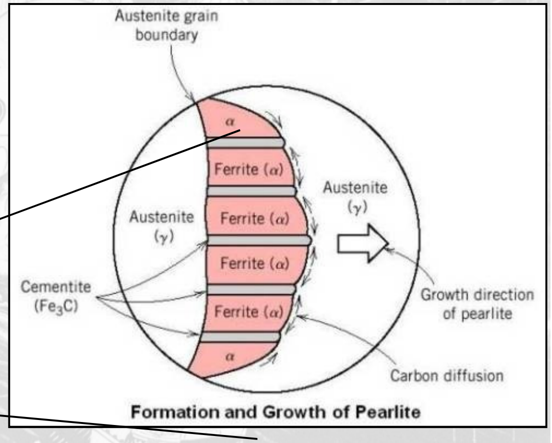

Austenite: the <u>soft</u> structure of steel at <u>high</u> temperature

Ferrite: the <u>soft</u> and <u>resilient</u> (almost) pure iron phase

Cementite: the <u>hard</u> and <u>brittle</u> carbon containing phase at <u>low</u> temperature

Pearlite: <u>hard</u> and <u>not</u> too much <u>brittle</u> mixture of <u>ferrite</u> and <u>cementite</u>

Metallurgy of steel

Metastable steel phase: martensite

Continuous cooling transformation

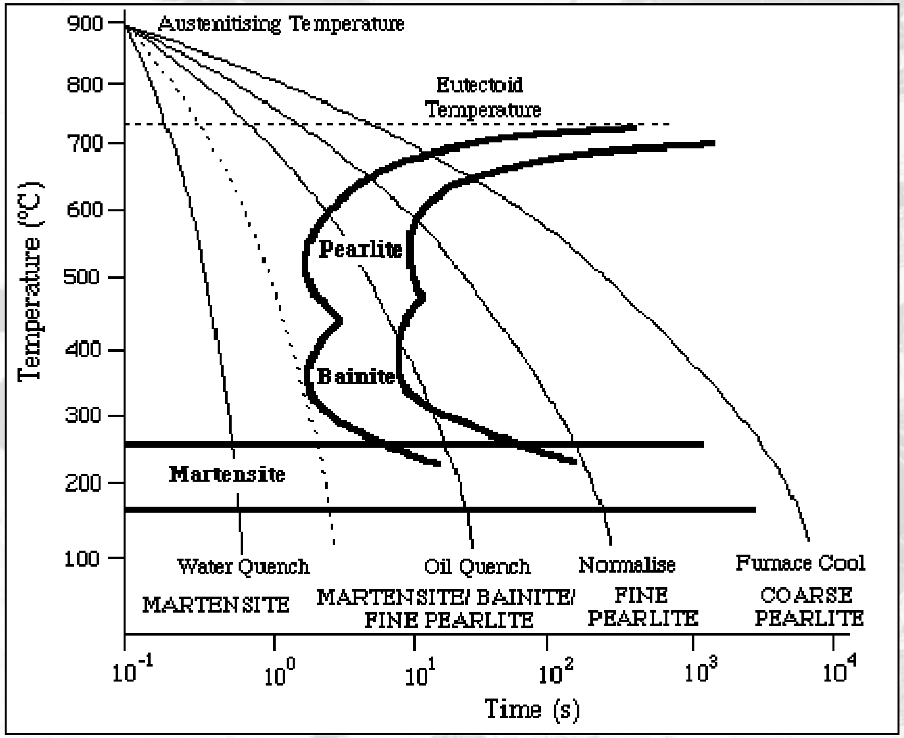

Direct transformation from austenite to martensite

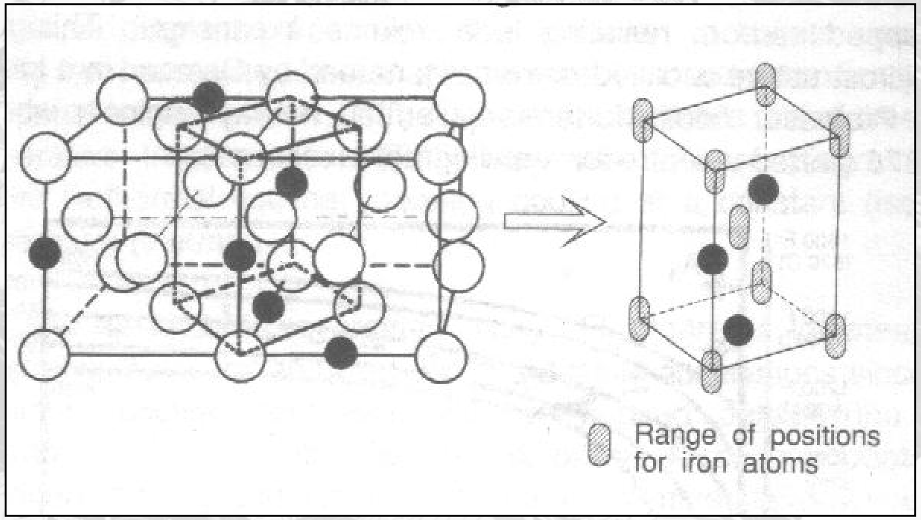

Fast cooling turns austenite into martensite (and ferrite)

Martensite: extremely hard and brittle metastable phase

Metallurgy of steel

Steel smelting

Two possible processes
(related to the available technology)

1) Bloomery iron (possibly steel)
- low temperature furnace (small size)
- low carbon enrichment
- solid state (metal and slag sponge)
- cheap method

2) Crucible steel
- high temperature furnace (large size)
- high carbon enrichment
- liquid state (slag removal)
- long and expensive process

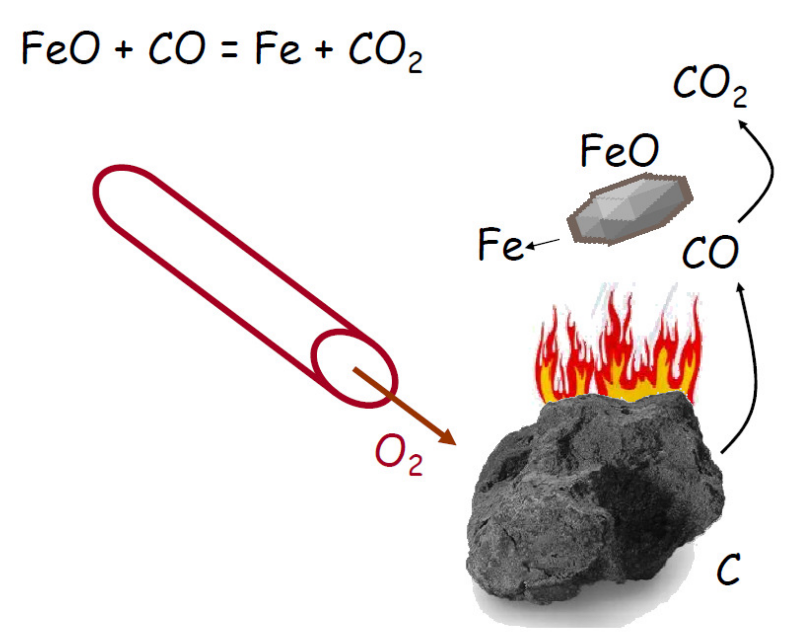

Slag inclusions are responsible for the brittleness of the material

Metallurgy of steel

Brittleness reduction:

Slag inclusion removal through mechanical action as lamination or pattern welding

Welding of brittle high carbon edges with resilient low carbon body

Tempering steel after martensitic transition

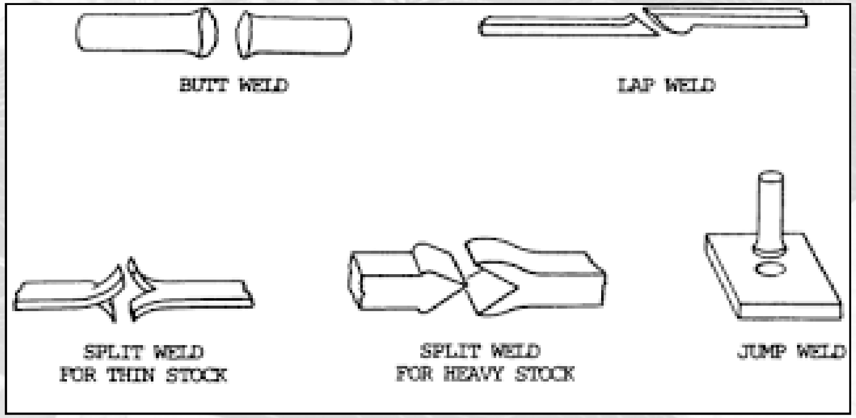

Neutron Imaging: principles

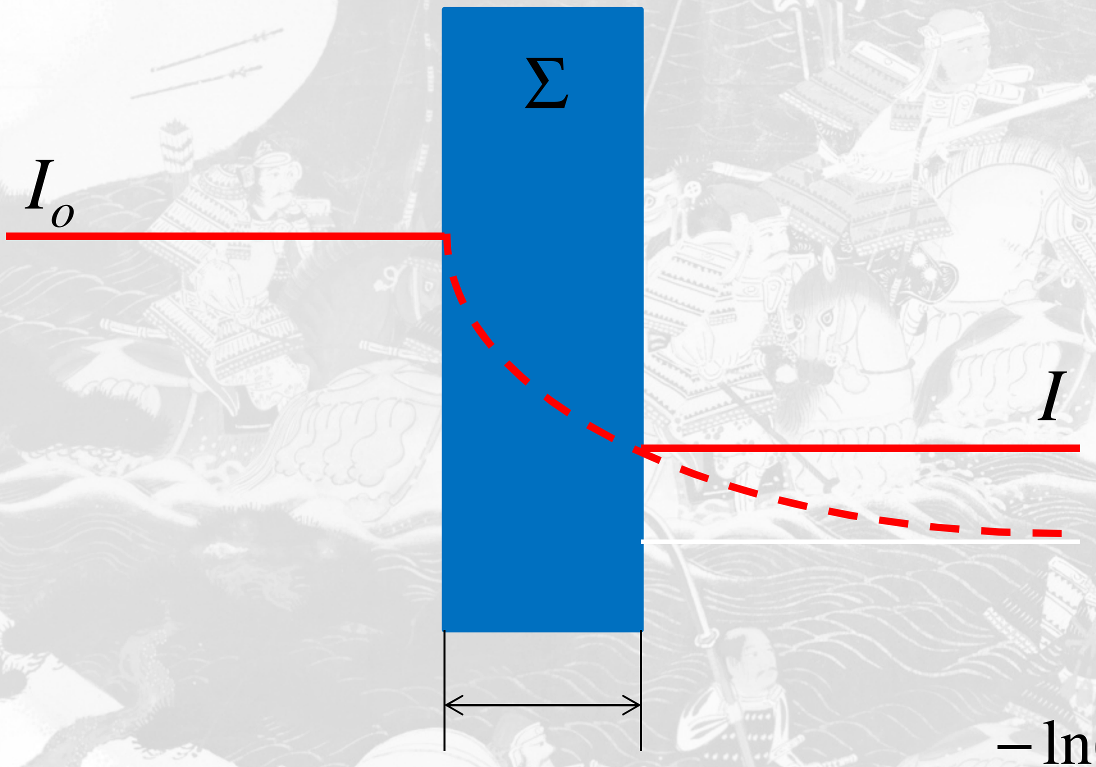

$$-\ln(T) = \Sigma d$$

$$I = I_0 e^{-\Sigma d} \qquad T = \frac{I}{I_0} \qquad \& \quad \Sigma = \sigma n$$

Lambert-Beer law

Trasmittance

Contrast:
material (σ) and thickness(d)

Complementary x-ray / neutron imaging results

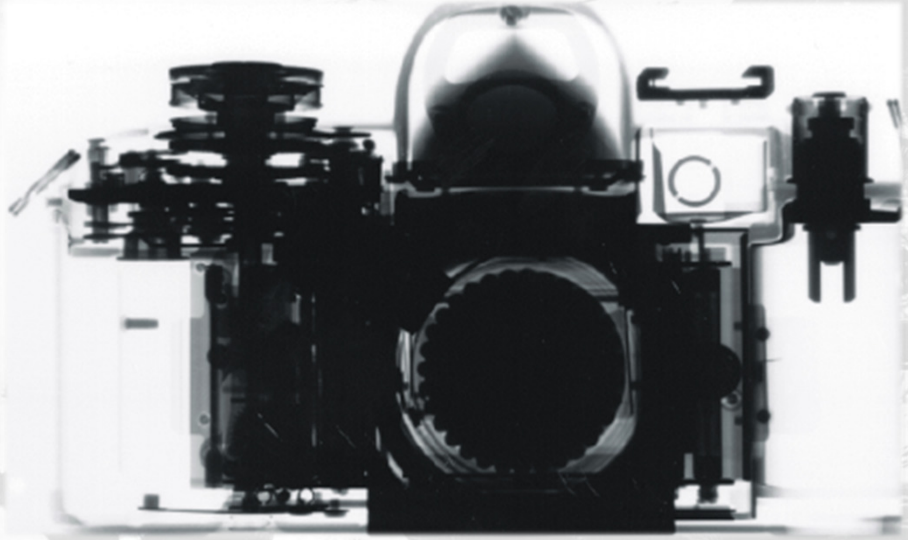

X-Ray

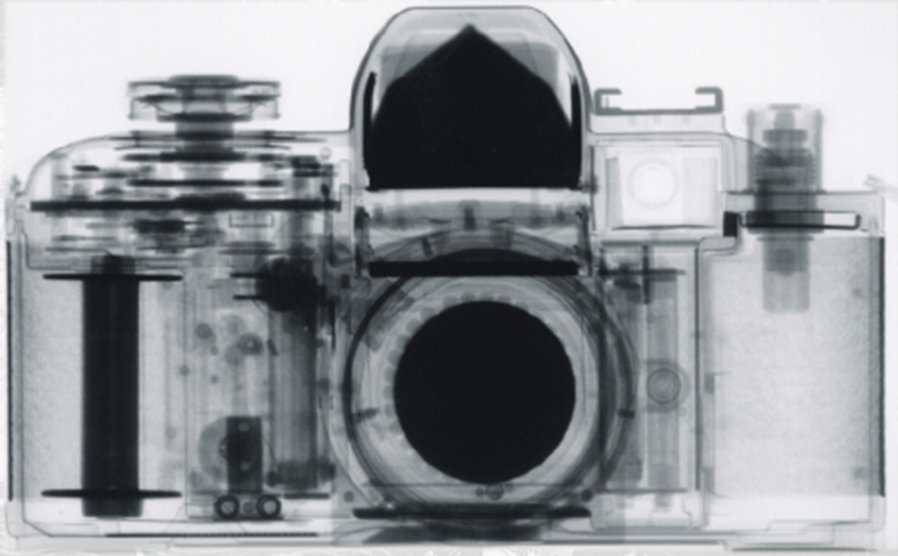

Neutron

Neutrons are optimal for:
-light elements,
-metals

Atomic Absorption cross sections

X Ray

Period ↓ / Group →	1	2	3	4	5	6	7	8	9	10	11	12	13	14	15	16	17	18
1	H 0.02																	He 0.02
2	Li 0.06	Be 0.22											B 0.28	C 0.27	N 0.11	O 0.16	F 0.14	Ne 0.17
3	Na 0.13	Mg 0.24											Al 0.38	Si 0.33	P 0.25	S 0.30	Cl 0.23	Ar 0.20
4	K 0.14	Ca 0.26	Sc 0.48	Ti 0.73	V 1.04	Cr 1.29	Mn 1.32	Fe 1.57	Co 1.78	Ni 1.96	Cu 1.97	Zn 1.64	Ga 1.42	Ge 1.33	As 1.50	Se 1.23	Br 0.90	Kr 0.73
5	Rb 0.47	Sr 0.86	Y 1.61	Zr 2.47	Nb 3.43	Mo 4.29	Tc 5.06	Ru 5.71	Rh 6.08	Pd 6.13	Ag 5.67	Cd 4.84	In 4.31	Sn 3.98	Sb 4.28	Te 4.06	I 3.45	Xe 2.53
6	Cs 1.47	Ba 2.73		Hf 19.70	Ta 25.47	W 30.49	Re 34.47	Os 37.92	Ir 39.01	Pt 38.61	Au 35.94	Hg 25.88	Tl 23.23	Pb 22.81	Bi 20.28	Po 20.22	At -	Rn 9.77
7	Fr -	Ra 11.80		Rf -	Db -	Sg -	Bh -	Hs -	Mt -	Ds -	Rg -	Uub -	Uut -	Uuq -	Uup -	Uuh -	Uus -	Uuo -
Lanthanides				La 5.04	Ce 5.79	Pr 6.23	Nd 6.46	Pm 7.33	Sm 7.68	Eu 5.66	Gd 8.69	Tb 9.46	Dy 10.17	Ho 10.17	Er 11.70	Tm 12.49	Yb 9.32	Lu 14.07
Actinides				Ac 24.47	Th 28.95	Pa 39.65	U 49.08	Np -	Pu -	Am -	Cm -	Bk -	Cf -	Es -	Fm -	Md -	No -	Lr -

Neutron

Period ↓ / Group →	1	2	3	4	5	6	7	8	9	10	11	12	13	14	15	16	17	18
1	H 3.44																	He 0.02
2	Li 3.30	Be 0.79											B 101.6	C 0.56	N 0.43	O 0.17	F 0.20	Ne 0.10
3	Na 0.09	Mg 0.15											Al 0.1	Si 0.11	P 0.12	S 0.06	Cl 1.33	Ar 0.03
4	K 0.06	Ca 0.08	Sc 2.00	Ti 0.60	V 0.72	Cr 0.54	Mn 1.21	Fe 1.19	Co 3.92	Ni 2.05	Cu 1.07	Zn 0.35	Ga 0.49	Ge 0.47	As 0.67	Se 0.73	Br 0.24	Kr 0.61
5	Rb 0.08	Sr 0.14	Y 0.27	Zr 0.29	Nb 0.40	Mo 0.52	Tc 1.76	Ru 0.58	Rh 10.88	Pd 0.78	Ag 4.04	Cd 115.1	In 7.58	Sn 0.21	Sb 0.30	Te 0.25	I 0.23	Xe 0.43
6	Cs 0.29	Ba 0.07		Hf 4.99	Ta 1.49	W 1.47	Re 6.85	Os 2.24	Ir 30.46	Pt 1.46	Au 6.23	Hg 16.21	Tl 0.47	Pb 0.38	Bi 0.27	Po -	At -	Rn -
7	Fr -	Ra 0.34		Rf -	Db -	Sg -	Bh -	Hs -	Mt -	Ds -	Rg -	Uub -	Uut -	Uuq -	Uup -	Uuh -	Uus -	Uuo -
Lanthanides				La 0.52	Ce 0.14	Pr 0.41	Nd 1.87	Pm 5.72	Sm 171.47	Eu 94.58	Gd 1479.0	Tb 0.93	Dy 32.42	Ho 2.25	Er 5.48	Tm 3.53	Yb 1.40	Lu 2.75
Actinides				Ac -	Th 0.59	Pa 8.46	U 0.82	Np 9.80	Pu 50.20	Am 2.86	Cm -	Bk -	Cf -	Es -	Fm -	Md -	No -	Lr -

Courtesy E. Lehmann – PSI(CH)

Instrumental set-up

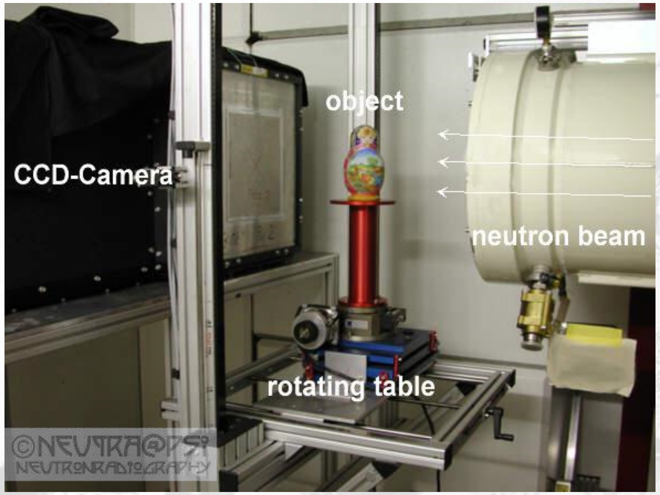

Andor DV 436 16-bit CCD Detector

2048×2048 pixels
nominal pixel size of 13.5 μm (CCD chip size: 2.76 cm x 2.76 cm)

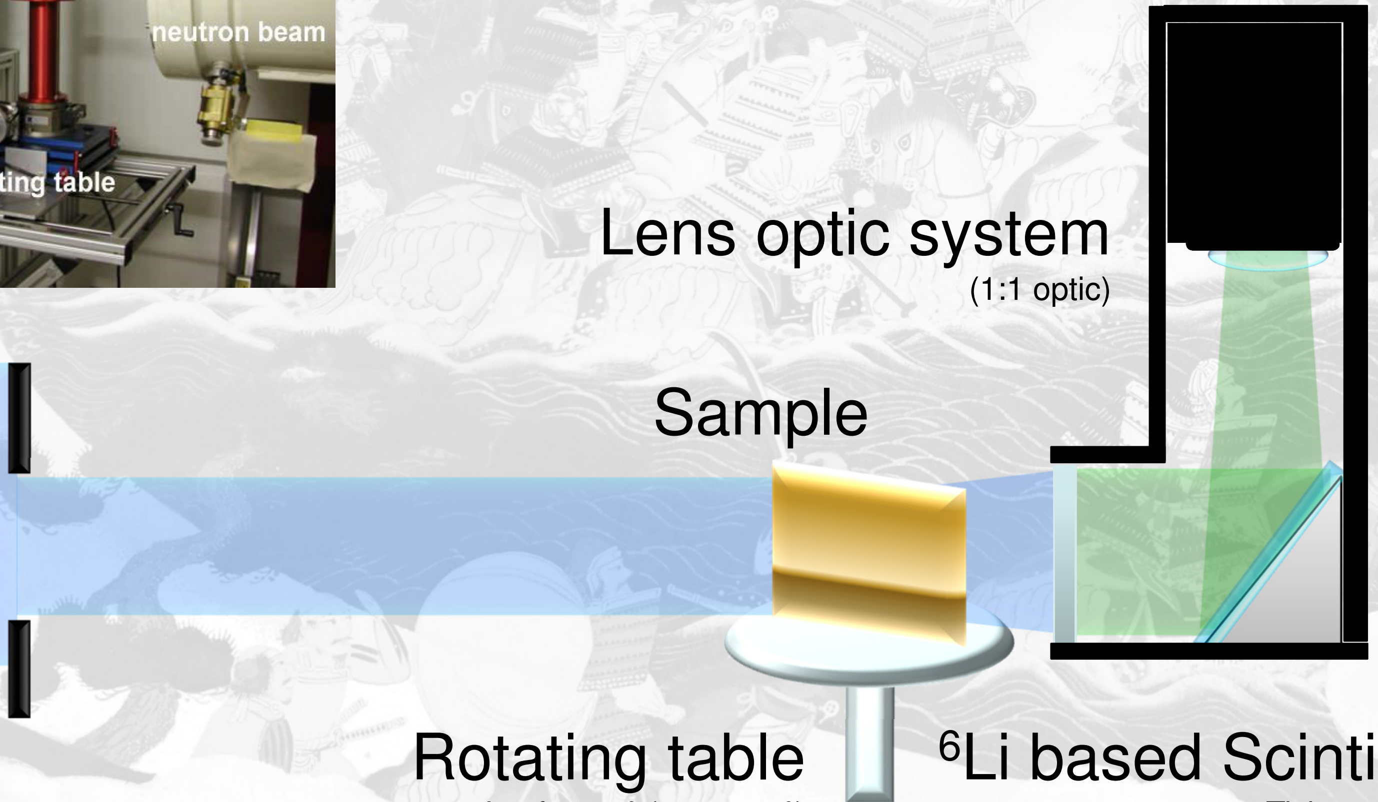

Lens optic system

(1:1 optic)

Sample

Pin hole

diameters: 4 cm
L/D achieved: 178

Rotating table

step angle of 0.96 ° (over 360°)
exposure time for projection: range from 5 s to 60 s

^{6}Li based Scintillator

Tickness: 100 μm

Computer tomography reconstruction

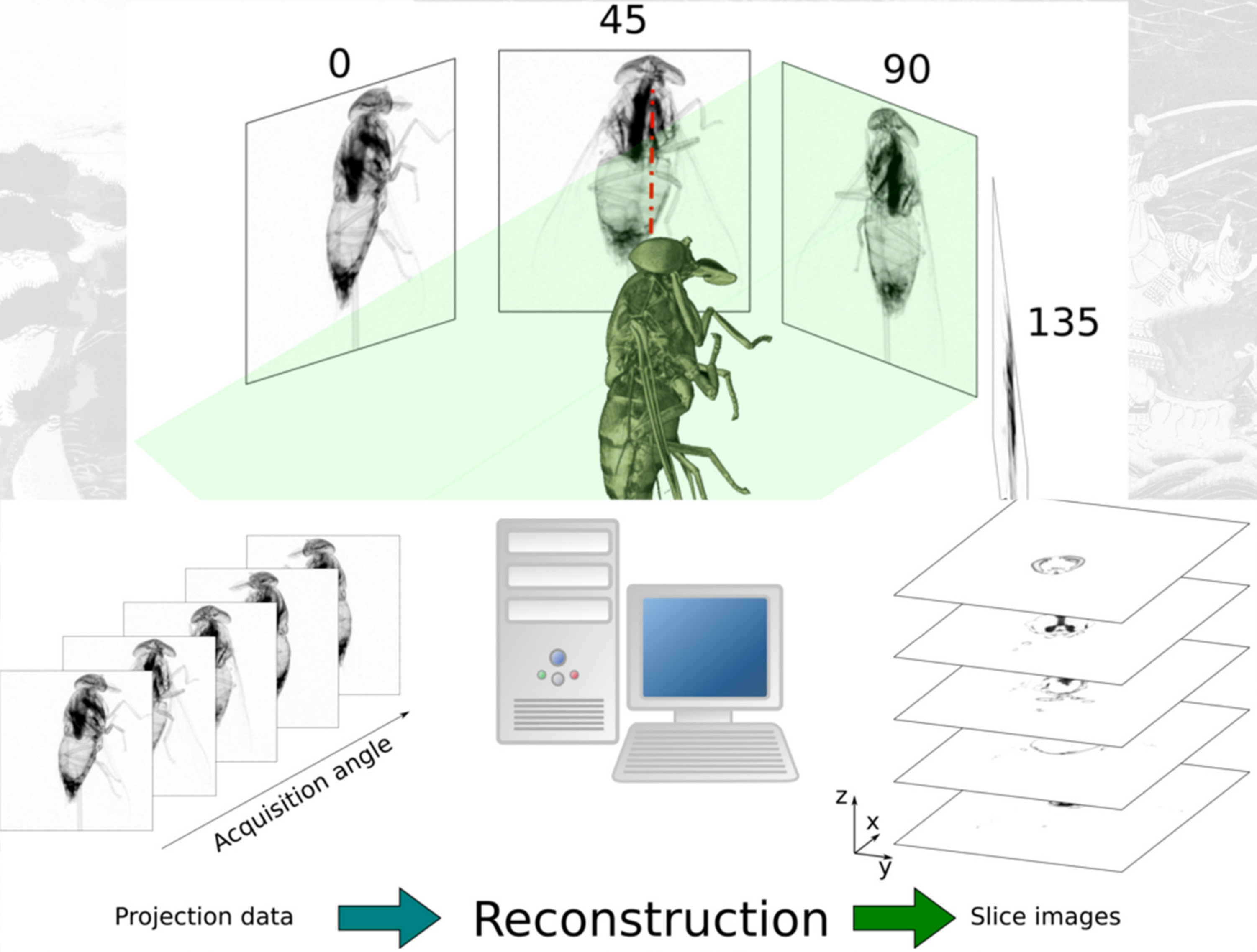

Energy selective neutron imaging (Bragg Edge transmission analysis)

polychromatic neutron beam

polycrystalline material

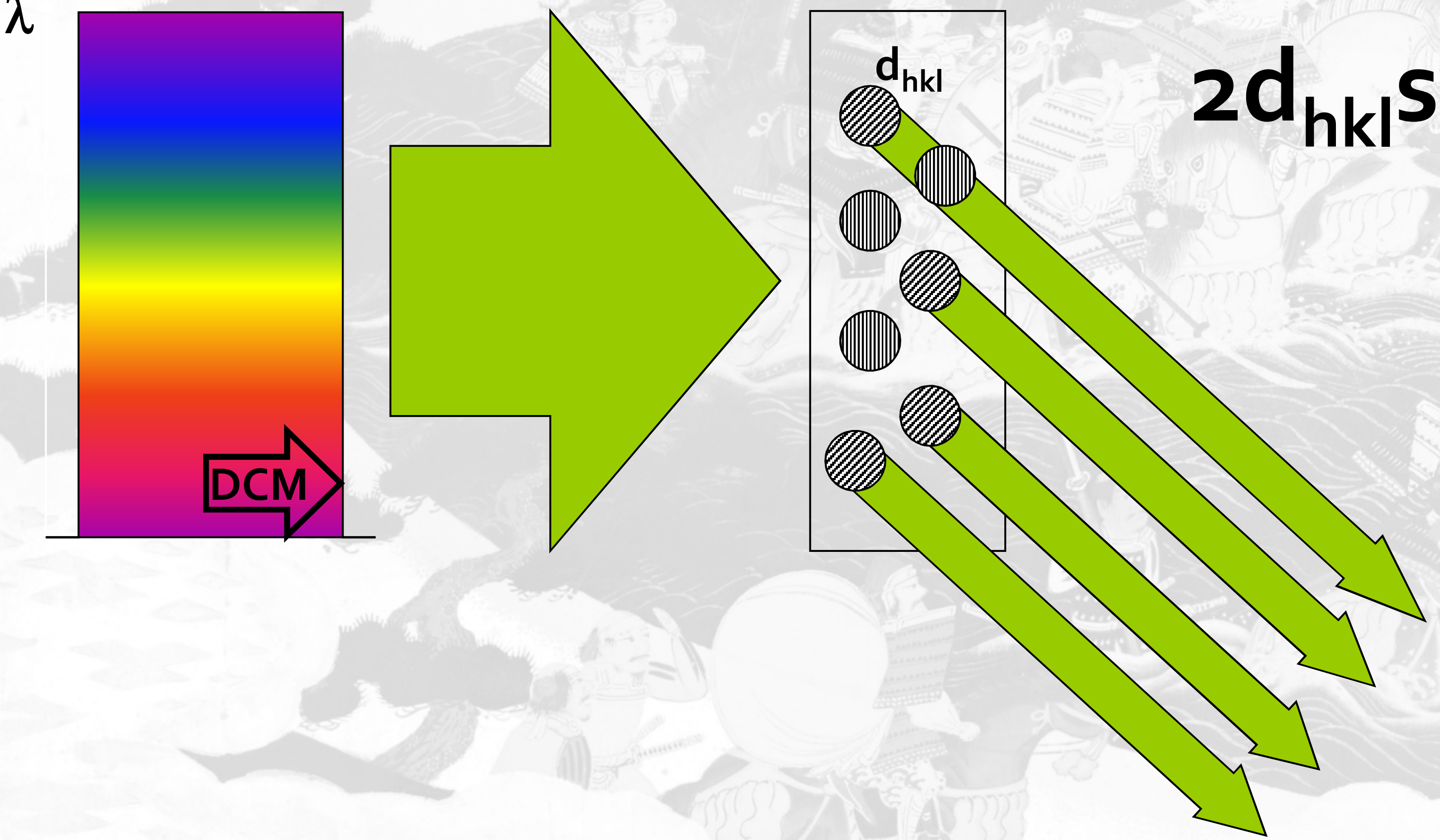

Bragg's law

$$2d_{hkl}\sin\theta=\lambda$$

Courtesy of Nikolay Kardjilov - Helmholtz-Zentrum Berlin für Materialien und Energie GmbH

Energy selective neutron imaging (Bragg Edge transmission analysis)

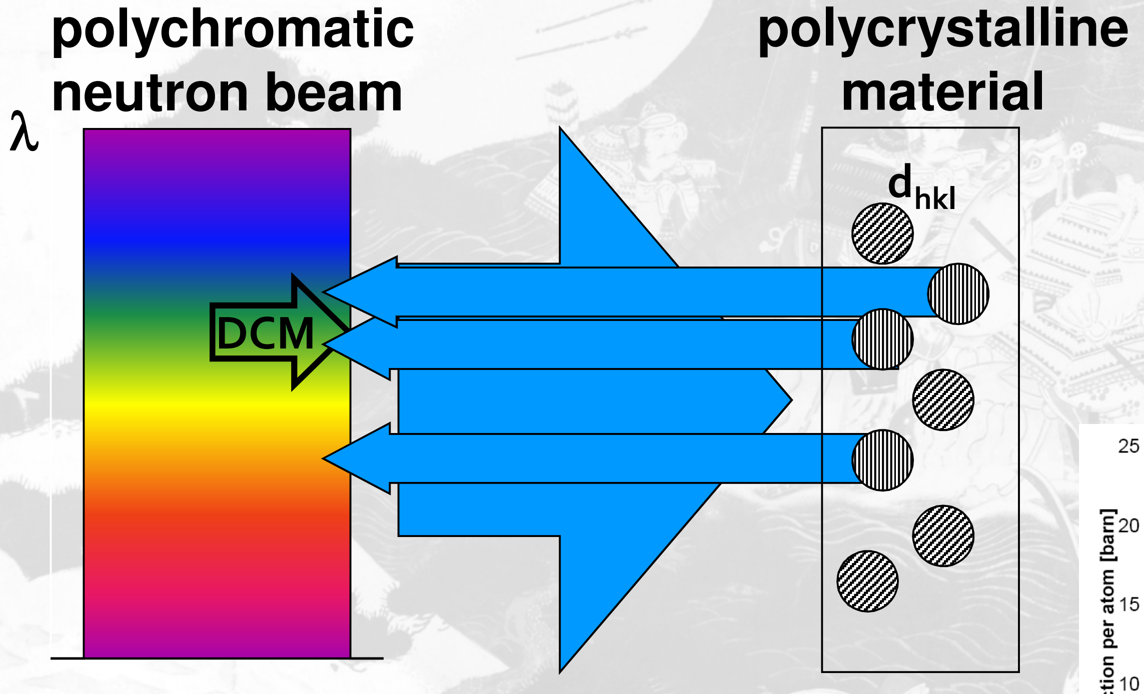

Bragg's law

$$2d_{hkl}\sin 90° = \lambda$$

Fe (bcc) transmission spectrum

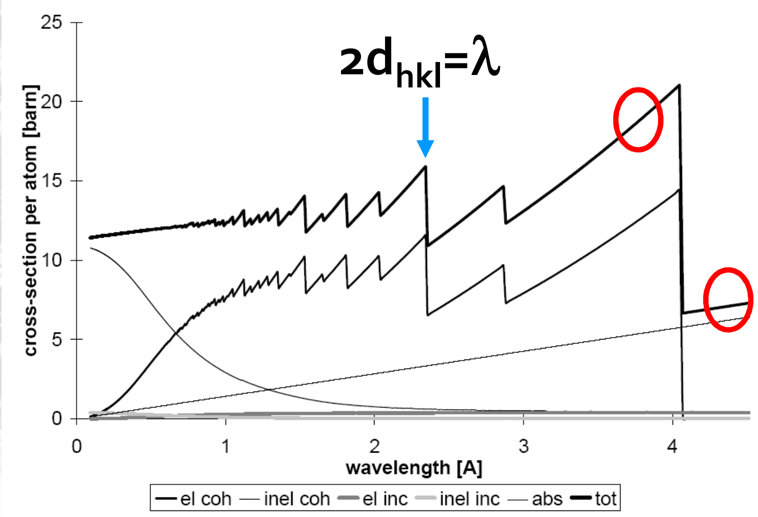

Courtesy of Nikolay Kardjilov - Helmholtz-Zentrum Berlin für Materialien und Energie GmbH

What neutron imaging can do

Morphological reconstruction of the inner structure and the components distribution

How?

White beam:

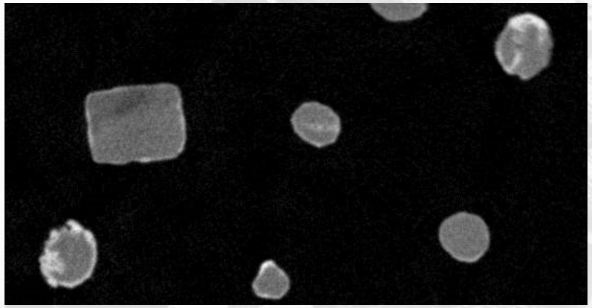

Different scattering and attenuation coefficient between metal and slags
(inclusions and welding lines)

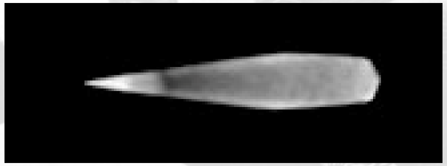

Different scattering power between martensite (fine grained) and the rest of steel
(quench hardened areas)

Energy selective:

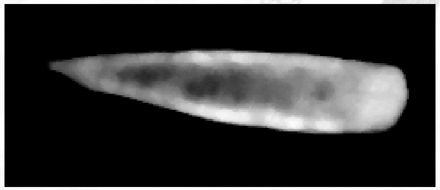

Different attenuation coefficient between high and low carbon steel
(different metal composition)

Armour pieces and swords examples

Japanese Helmets

Chronology

Ancient Period (*jōdai*; VIII secolo-1532)

Middle Ages (*chūko*; 1532-1614)

Modern Era (*kindai*; 1614-1868)

Typologies

Horagai Bachi helmet

The helmet was supposed to be made of a single folded sheet of iron

Results

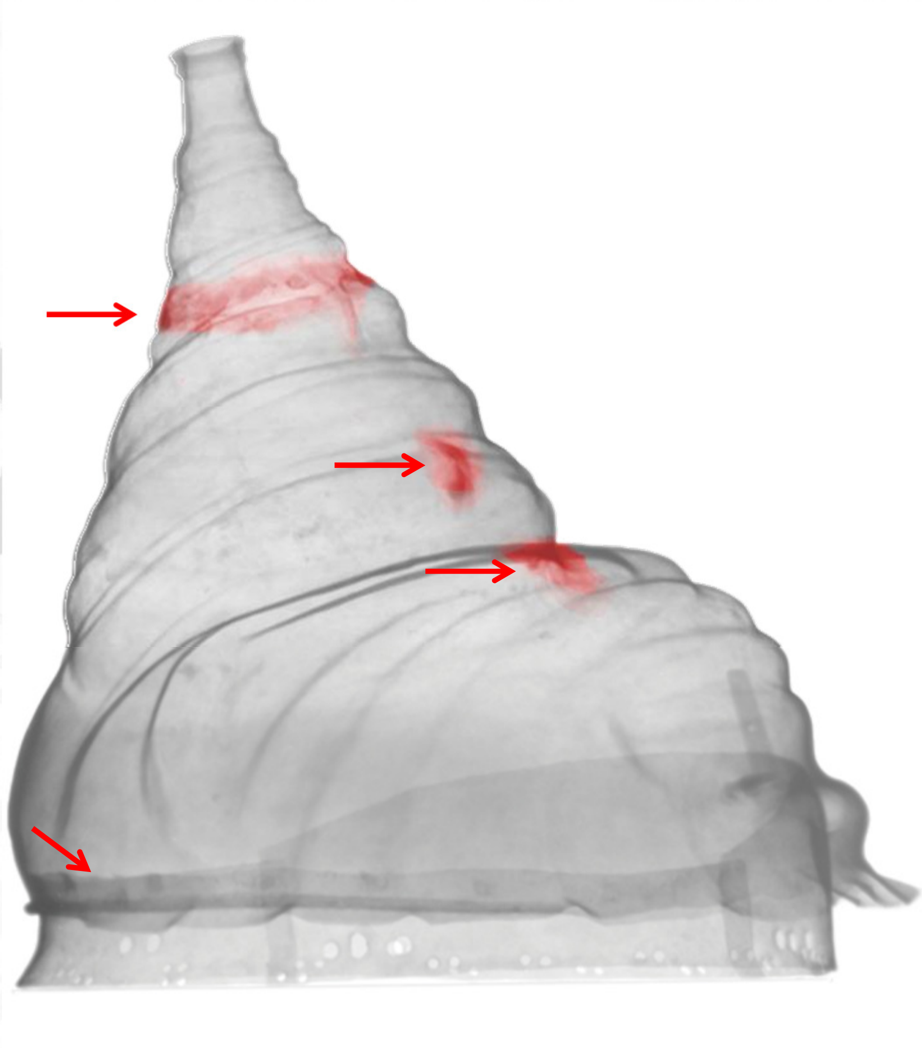

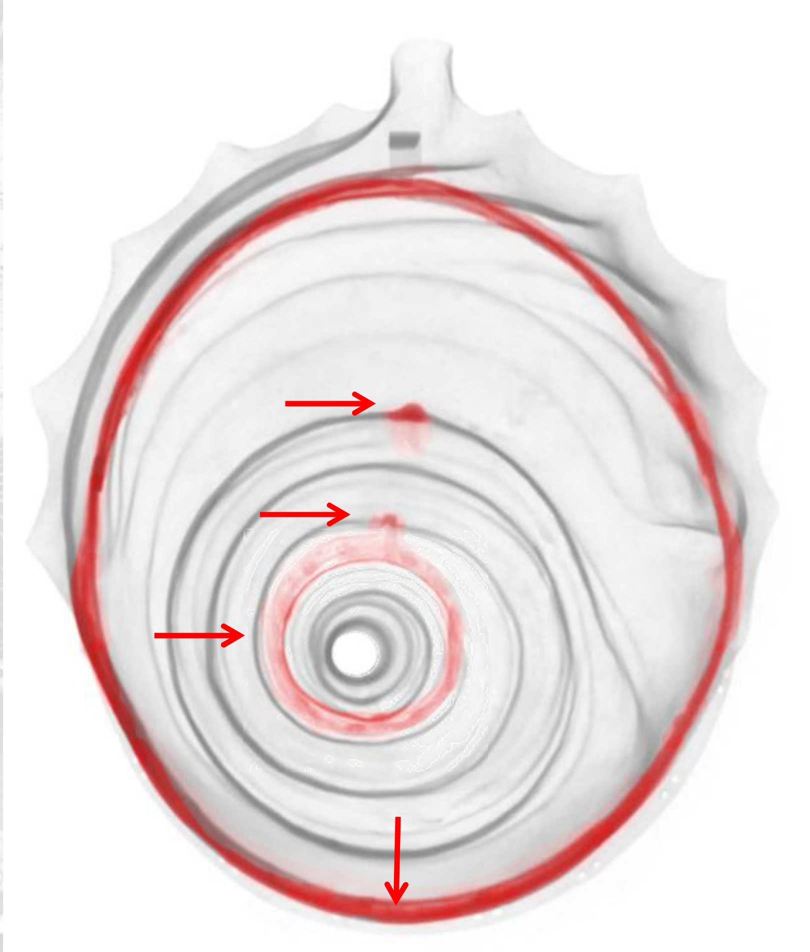

Suji-Bachi helmet

The helmet has a complex lamellar structure with no visible external riveting: how was it assembled?

Results

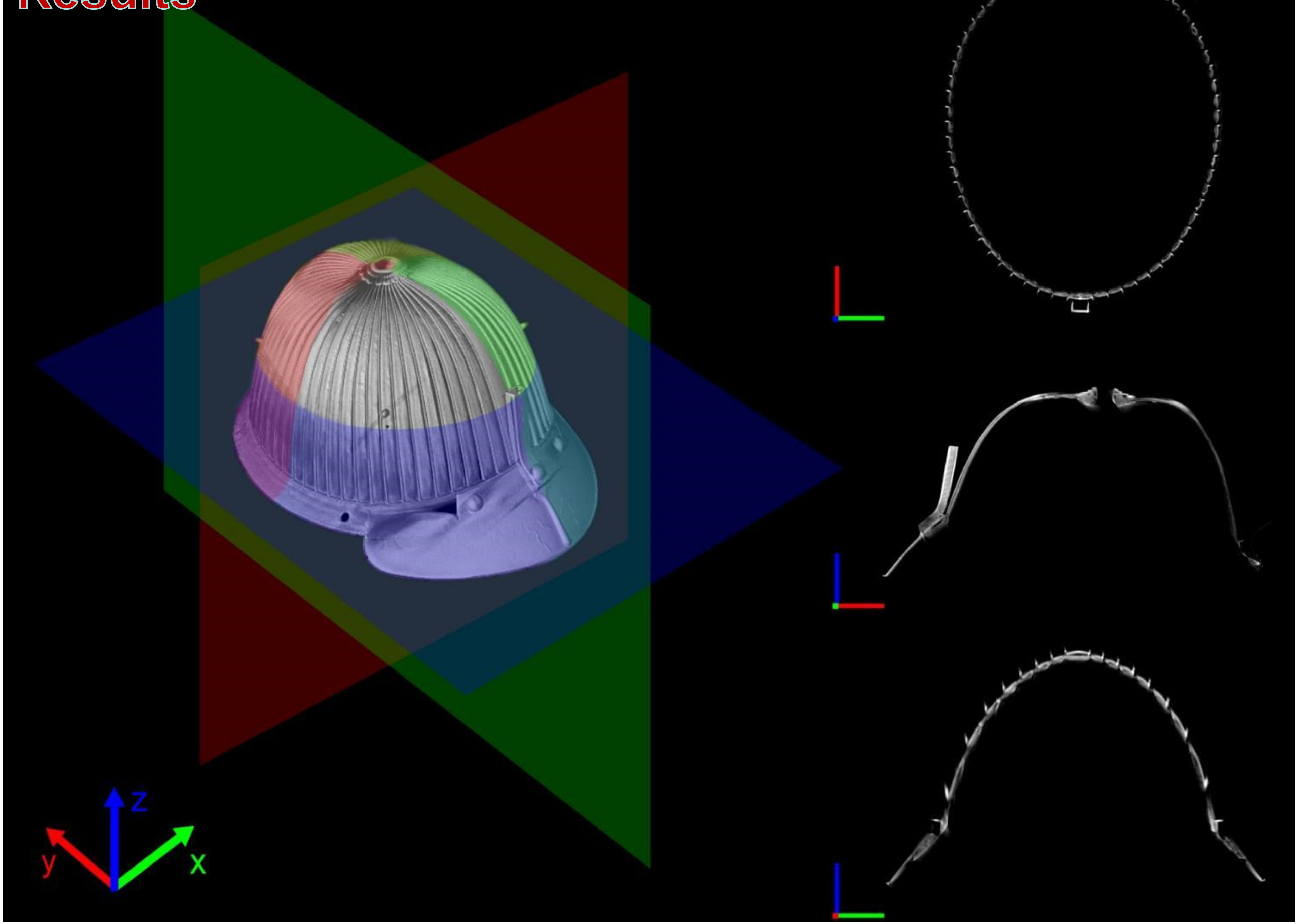

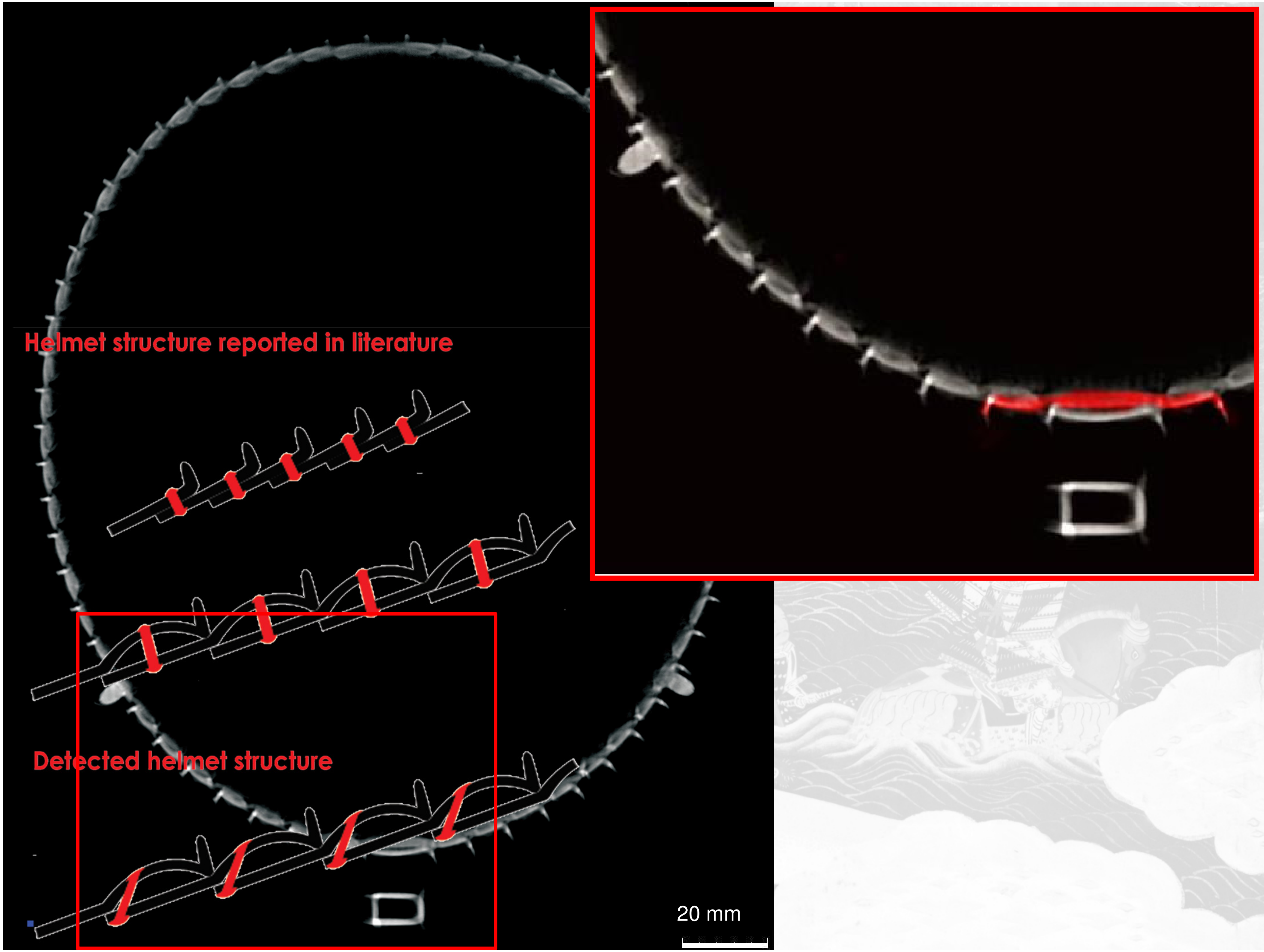

Helmet structure reported in literature
Detected helmet structure
20 mm

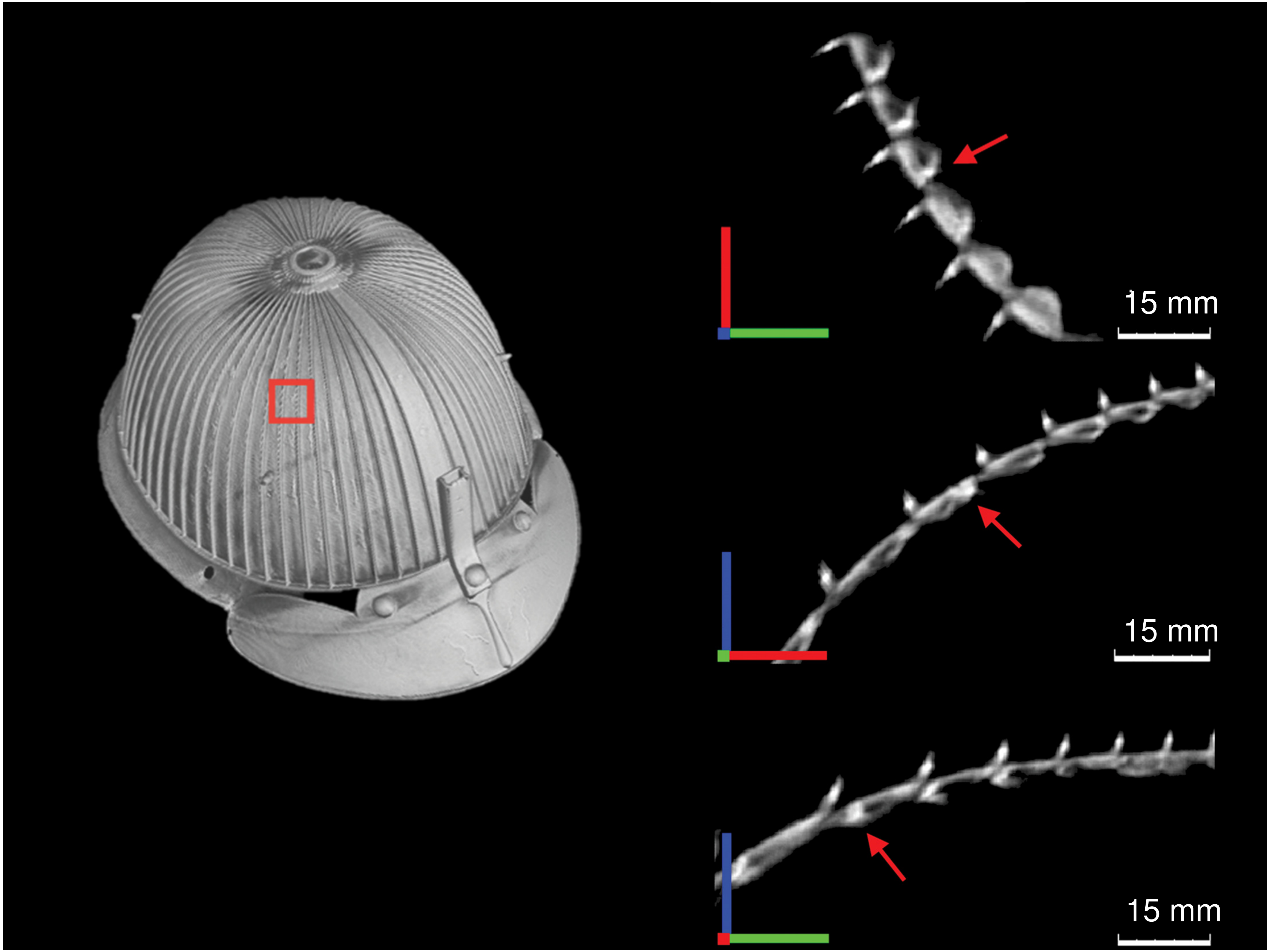
15 mm
15 mm
15 mm

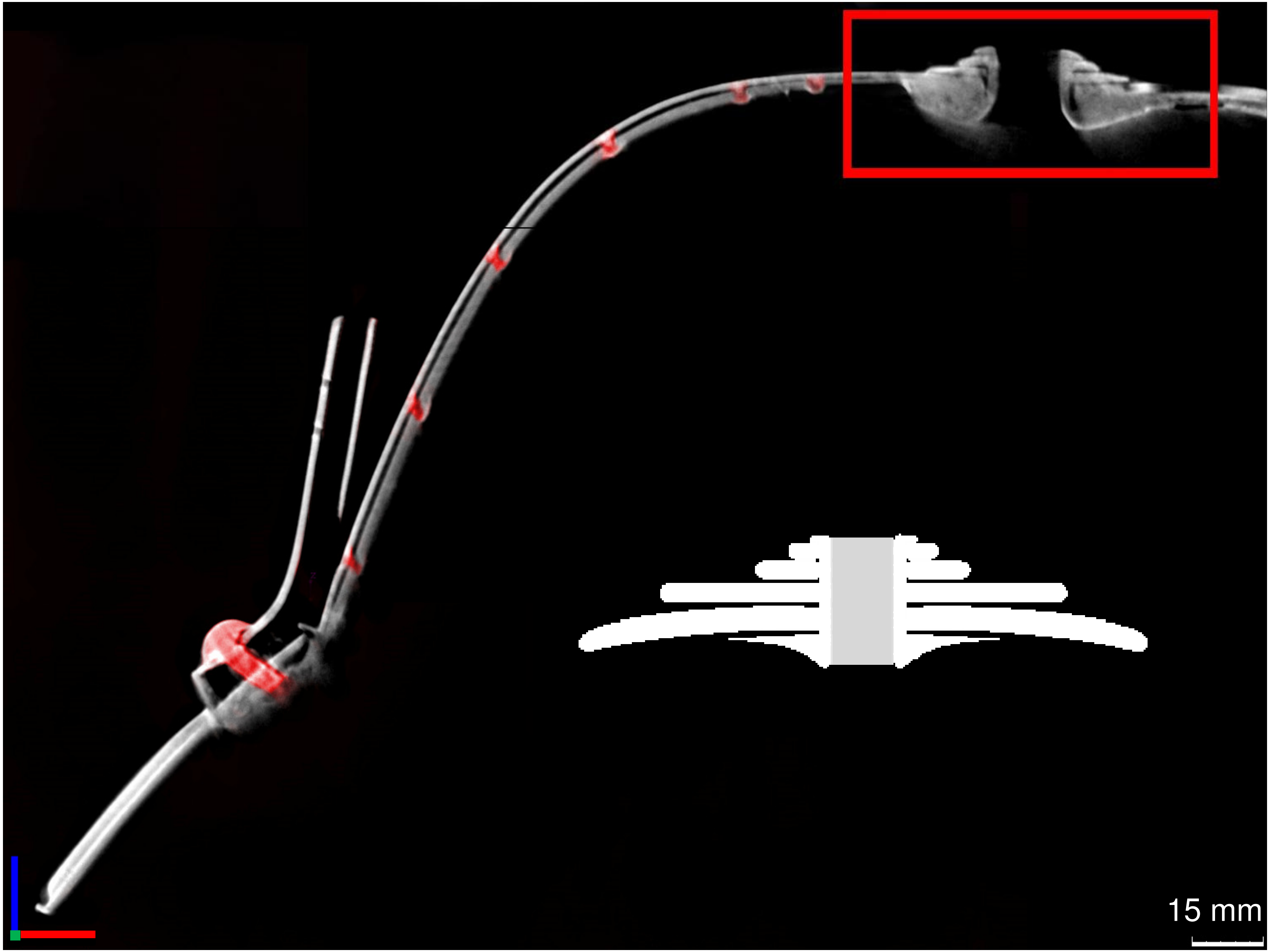
15 mm

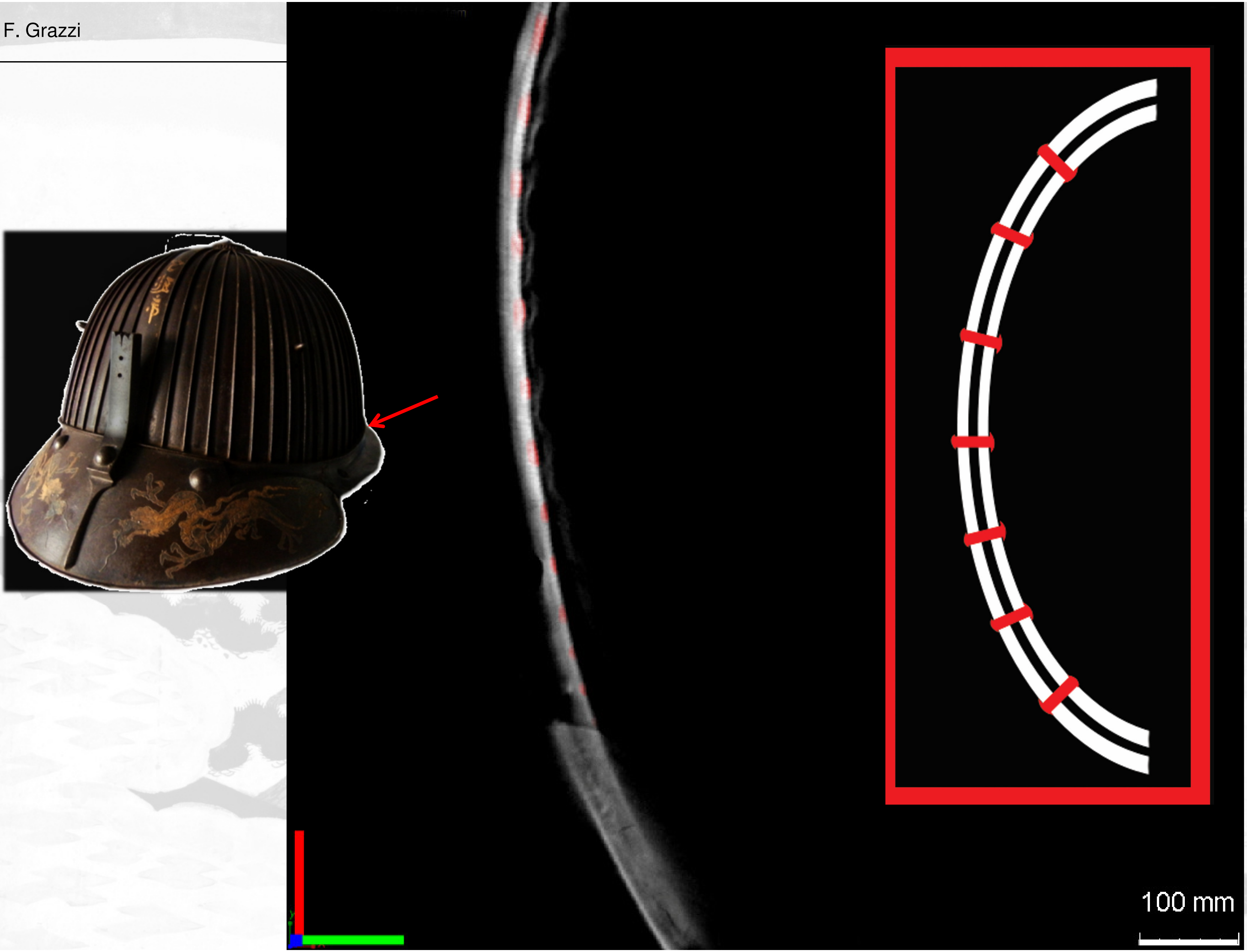
100 mm

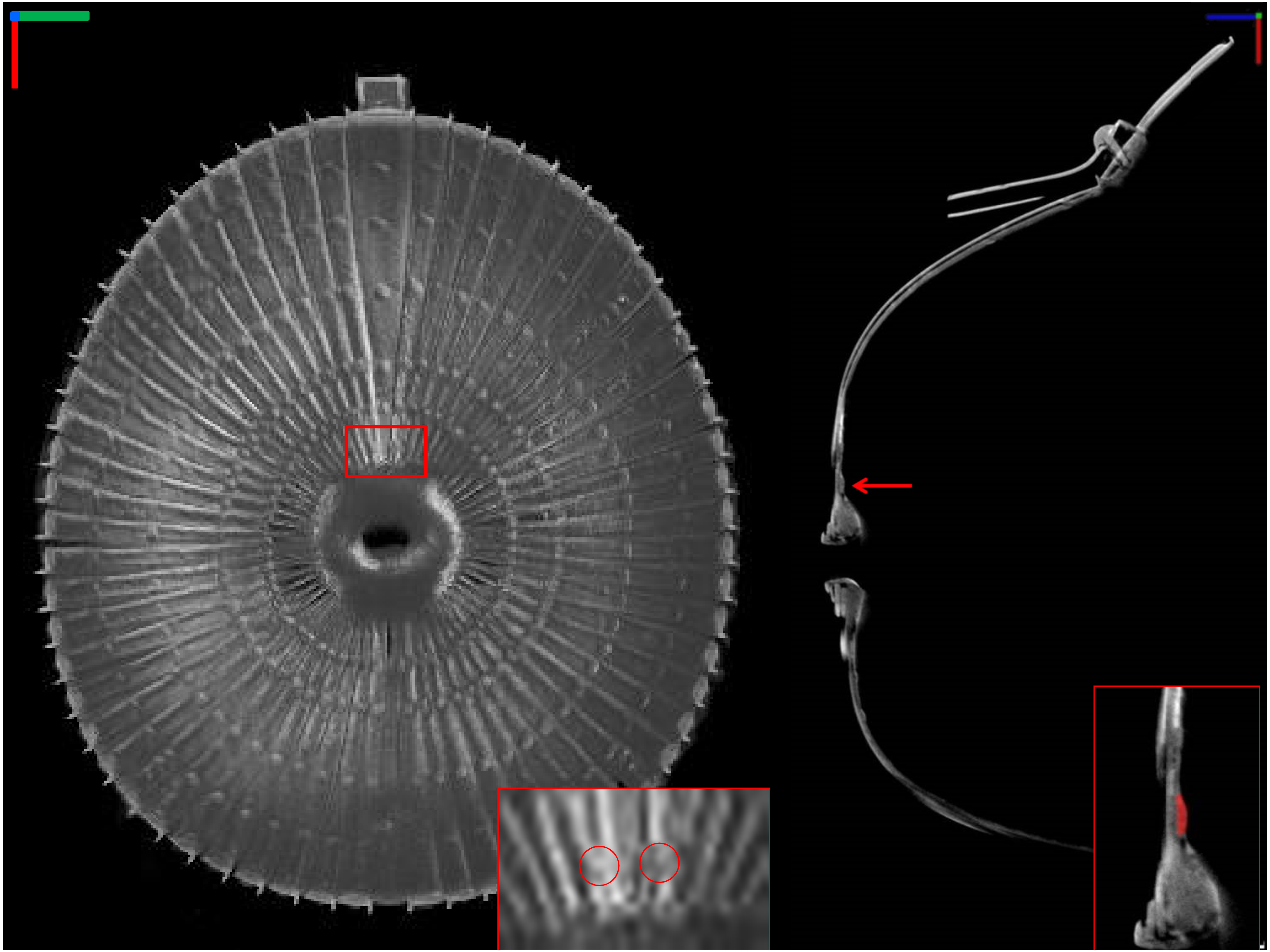

European 17th Century swords

Toledo swords were overprized on any other (factor up to 3!)

Made in Solingen (Germany)

Made in Toledo (Spain)

Selection of two groups: Spanish swords, German swords

Identification of the qualitative factors responsible for this evaluation

European 17th Century swords: HE4 – Solingen

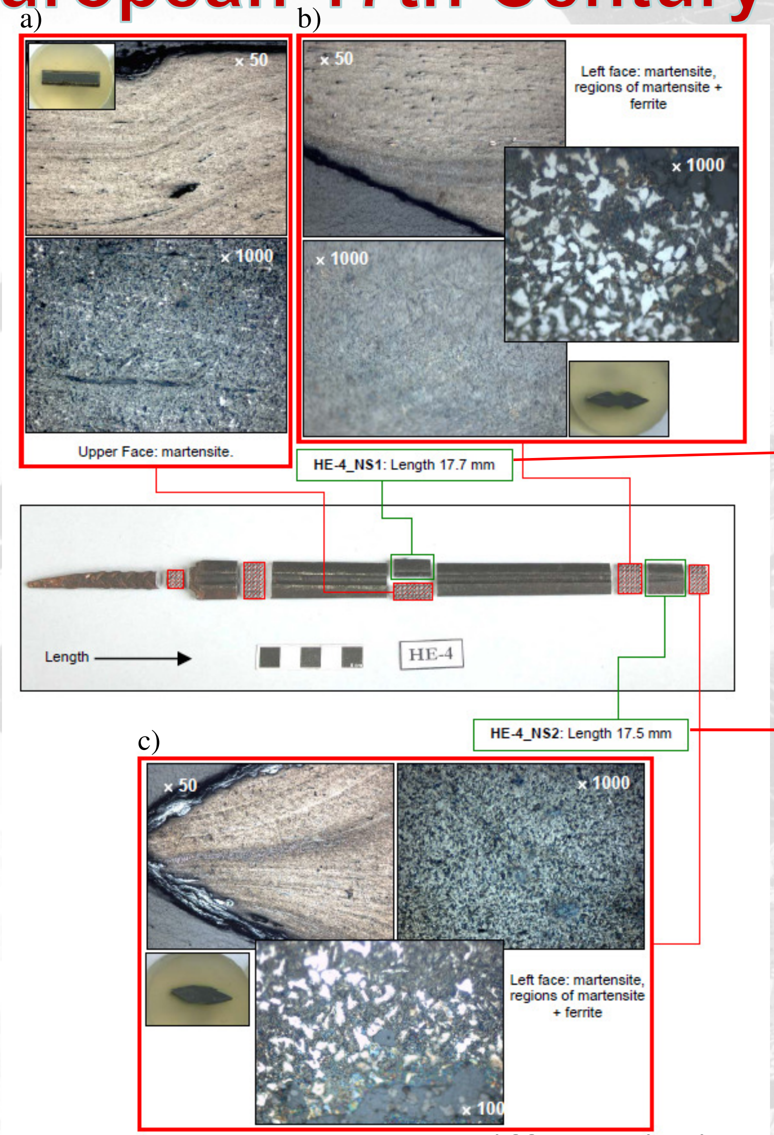

welding

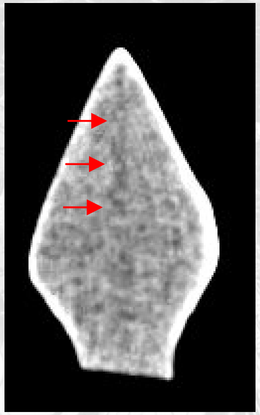

HE4 – NS1

slag inclusions

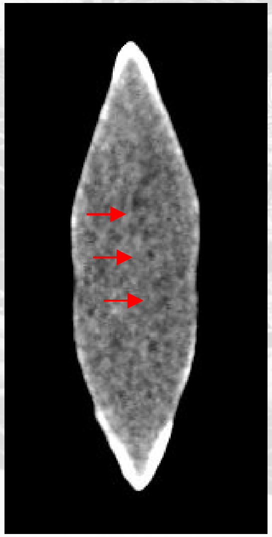

HE4 – NS2

<u>no phase differentiation: homogeneous sample</u>

European 17th Century swords: HE5 – Toledo

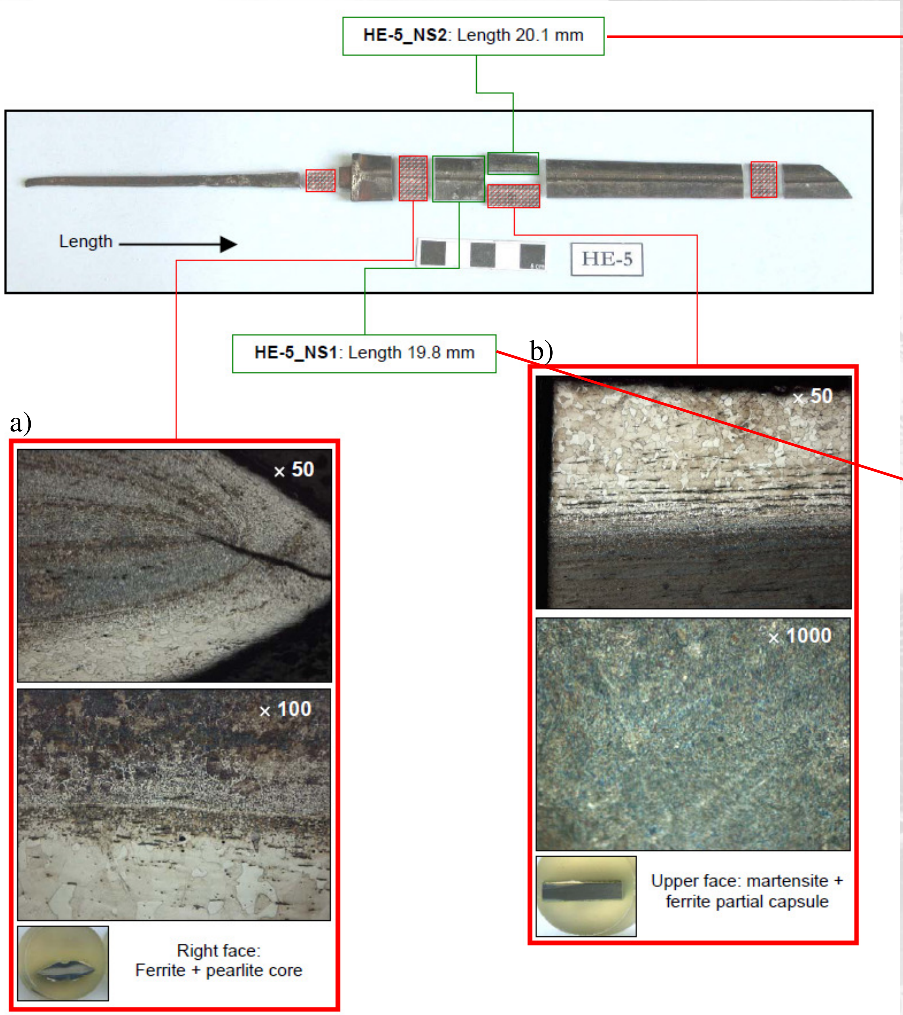

low carbon areas

phase differentiation: differently distributed steel

Danish 9th-11th Century Viking swords

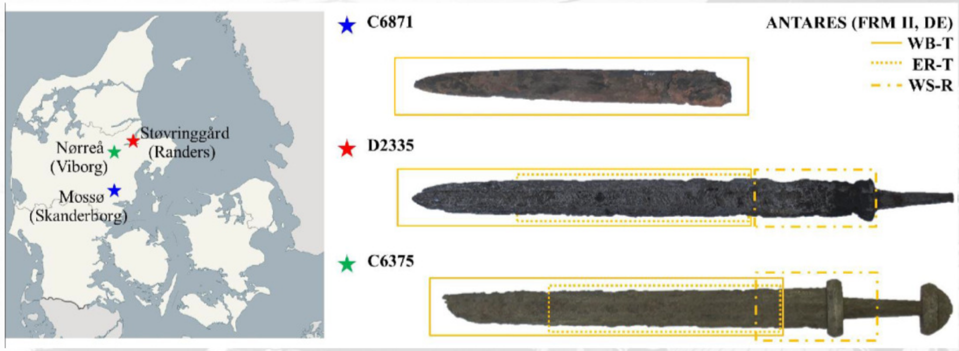

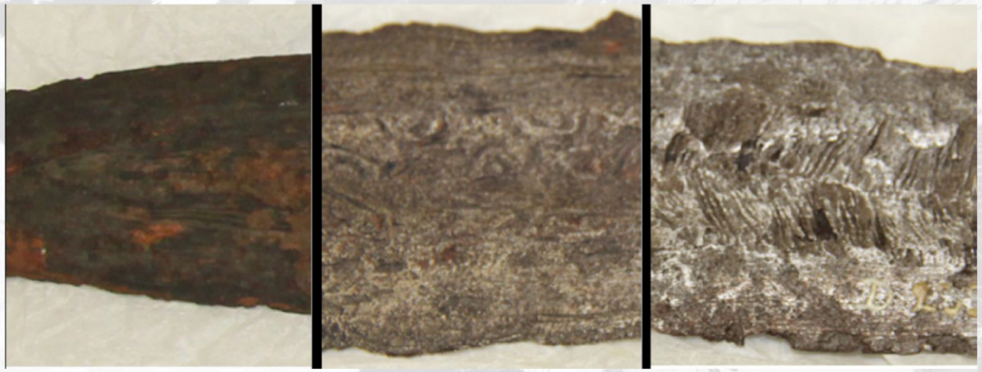

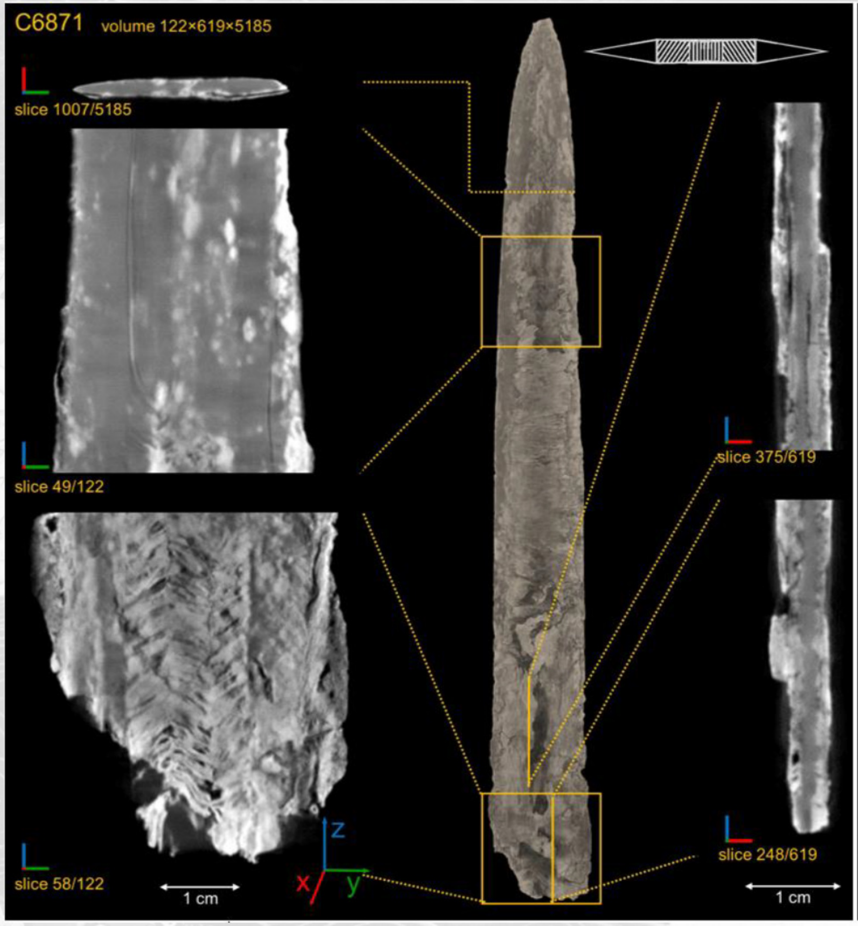

Inclusions and corrosion products are mapped
Pattern welding structure mapped

Niels Bohr Institutet

FRM II
Forschungs-Neutronenquelle
Heinz Maier-Leibnitz

Structure of pattern welded Viking swords

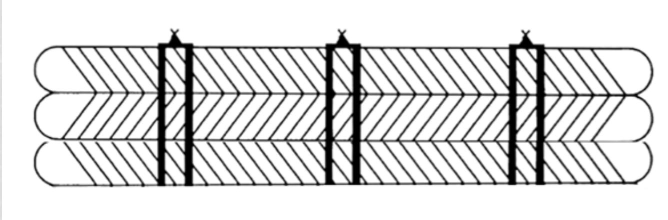

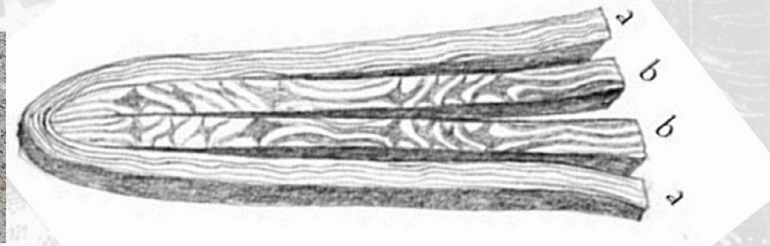

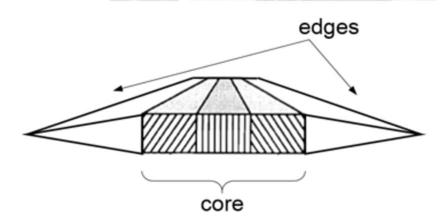

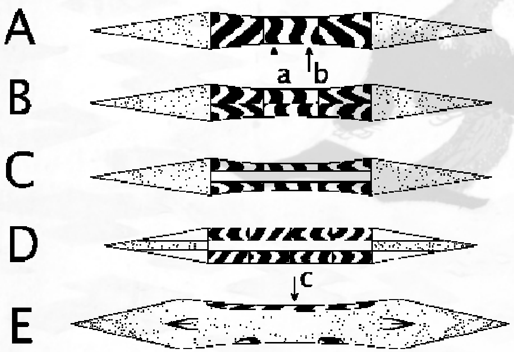

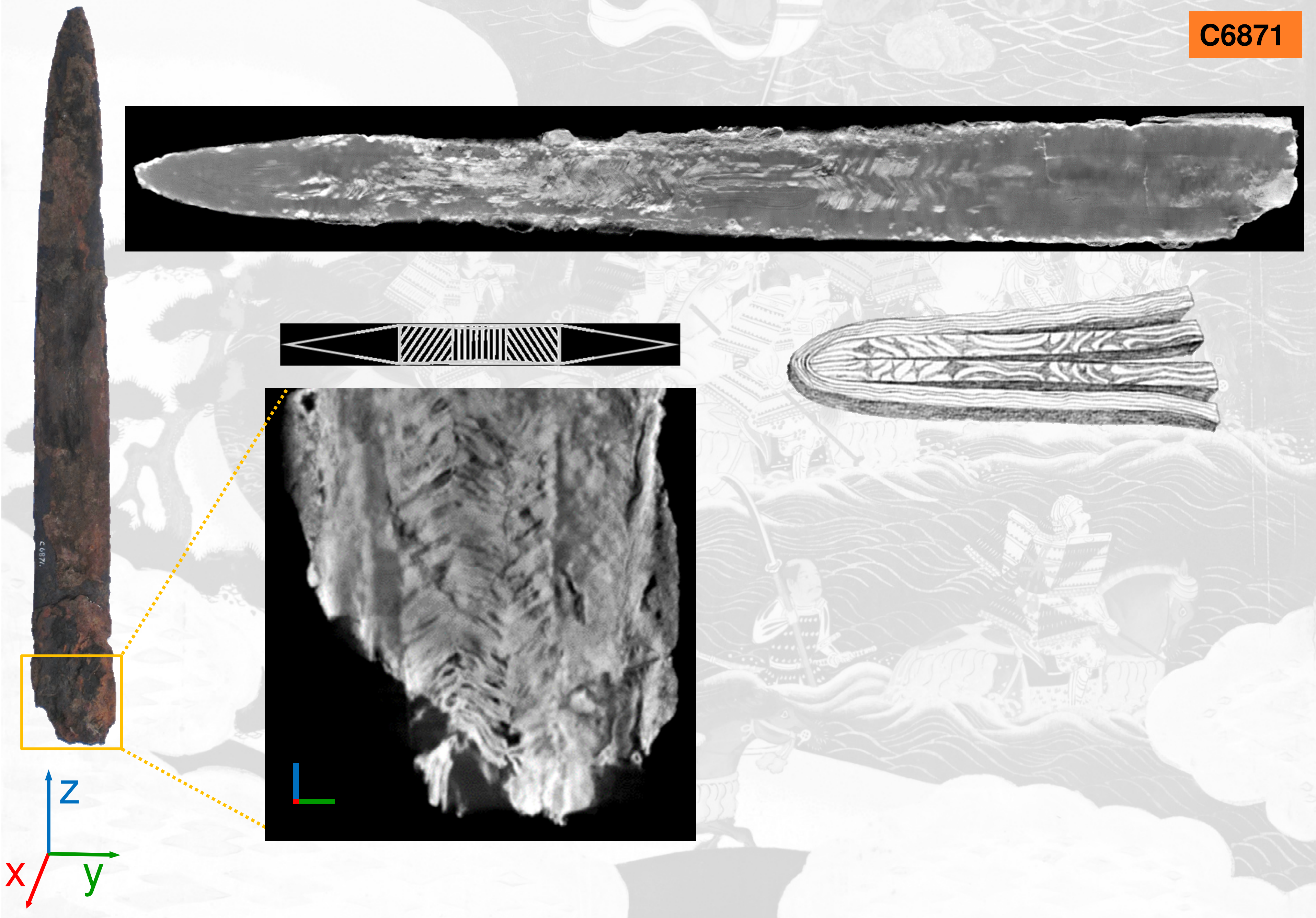
C6871
z
x
y

C6375

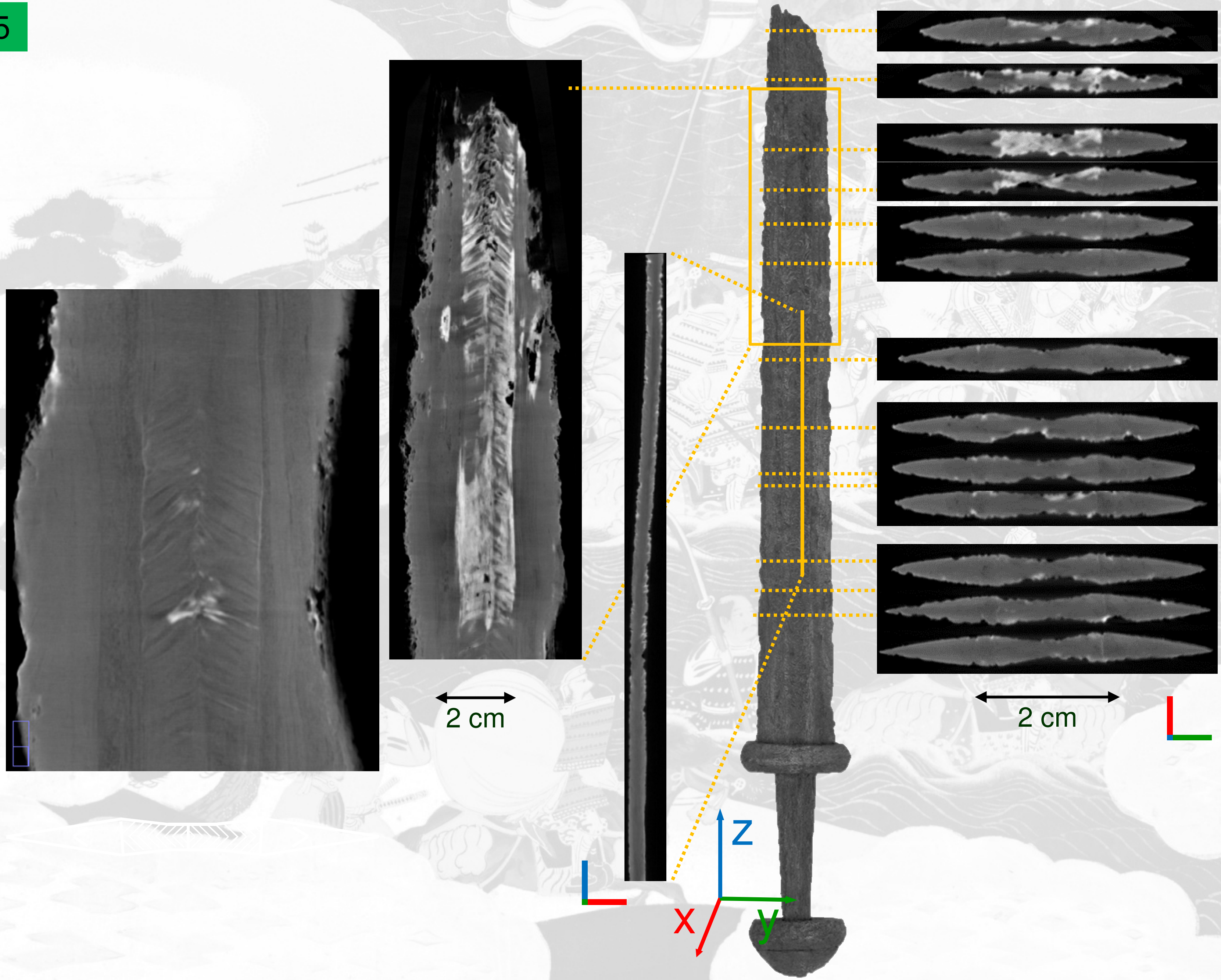

C6375

$$\ln\left[\frac{I(\lambda_1)}{I(\lambda_2)}\right]$$

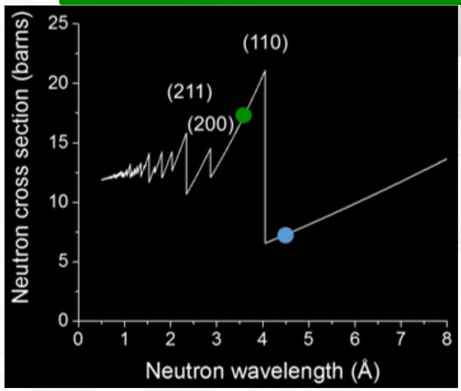

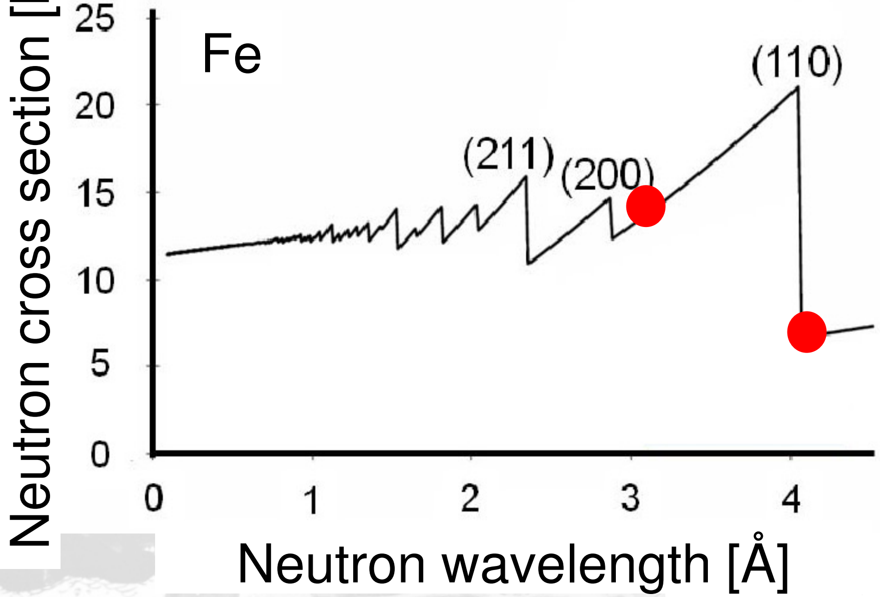
Fe
Neutron cross section [barns]
Neutron wavelength [Å]
(110)
(211)
(200)
25
20
15
10
5
0
0
1
2
3
4

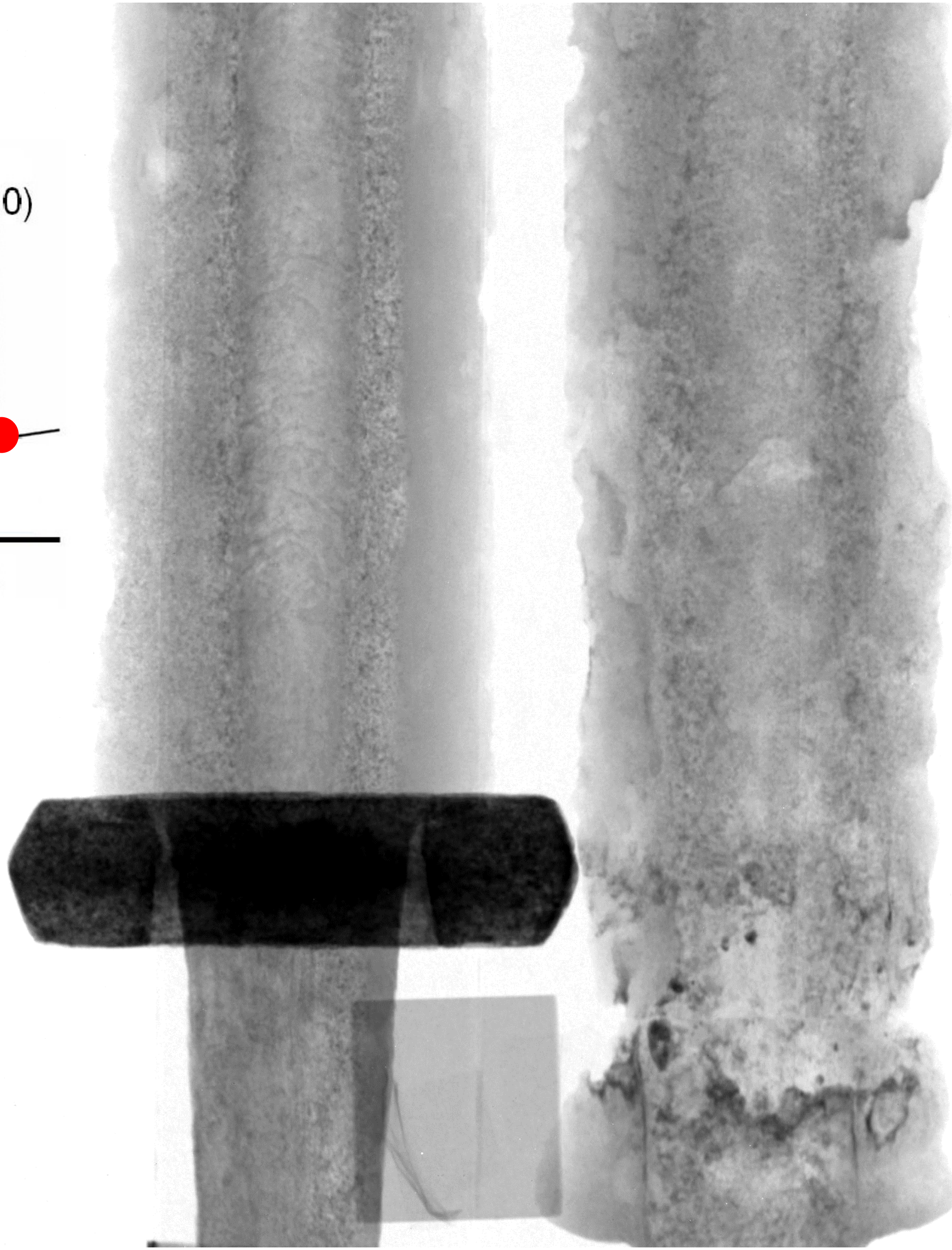

Kris, weapon of the Malay world

K1

K4

K2

K3

Storia Naturale
Museo di
Università degli Studi di Firenze

HELMHOLTZ ZENTRUM BERLIN
für Materialien und Energie

Making a kris

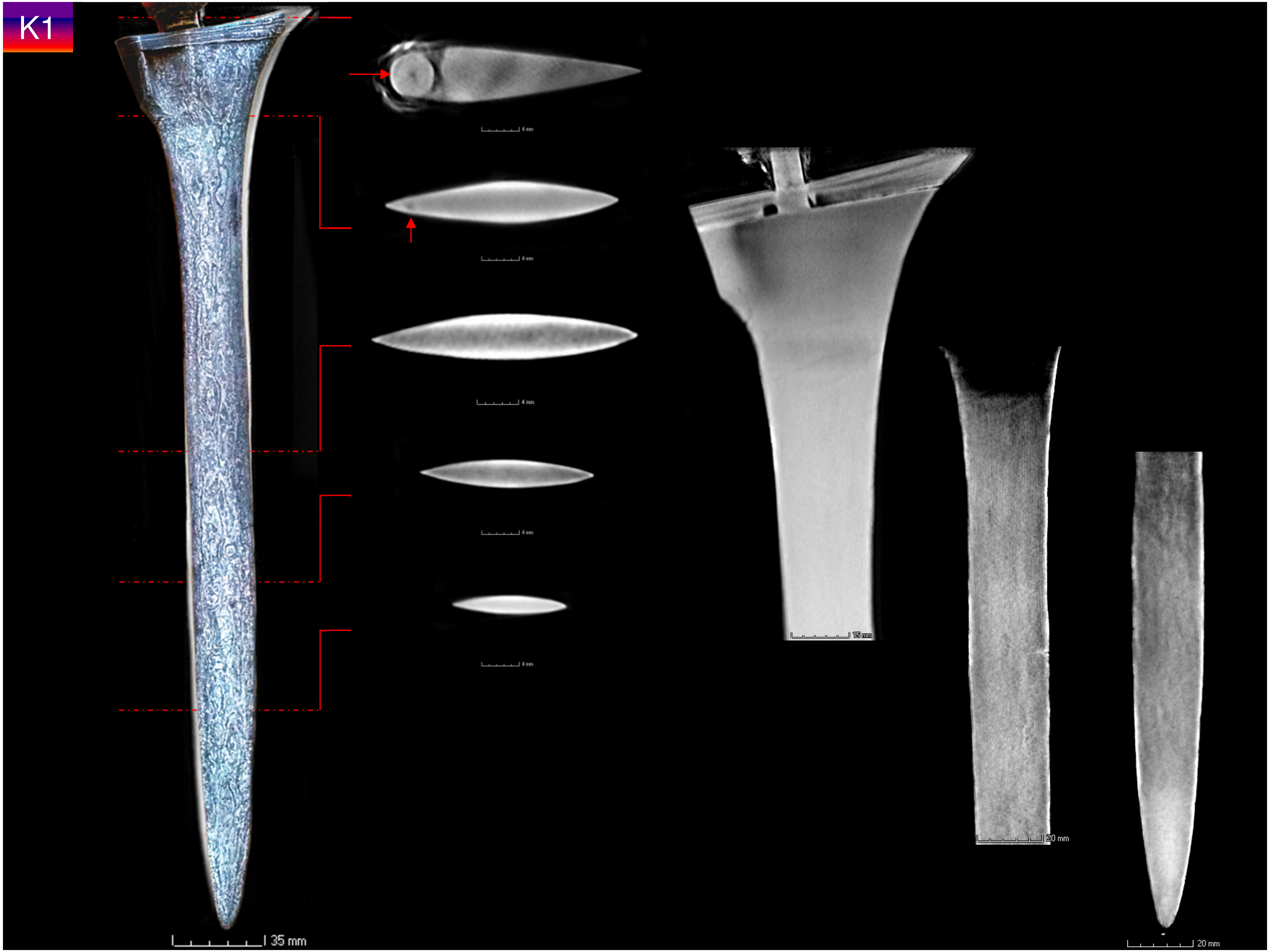

K1
35 mm
4 mm
4 mm
4 mm
4 mm
4 mm
15 mm
20 mm
20 mm

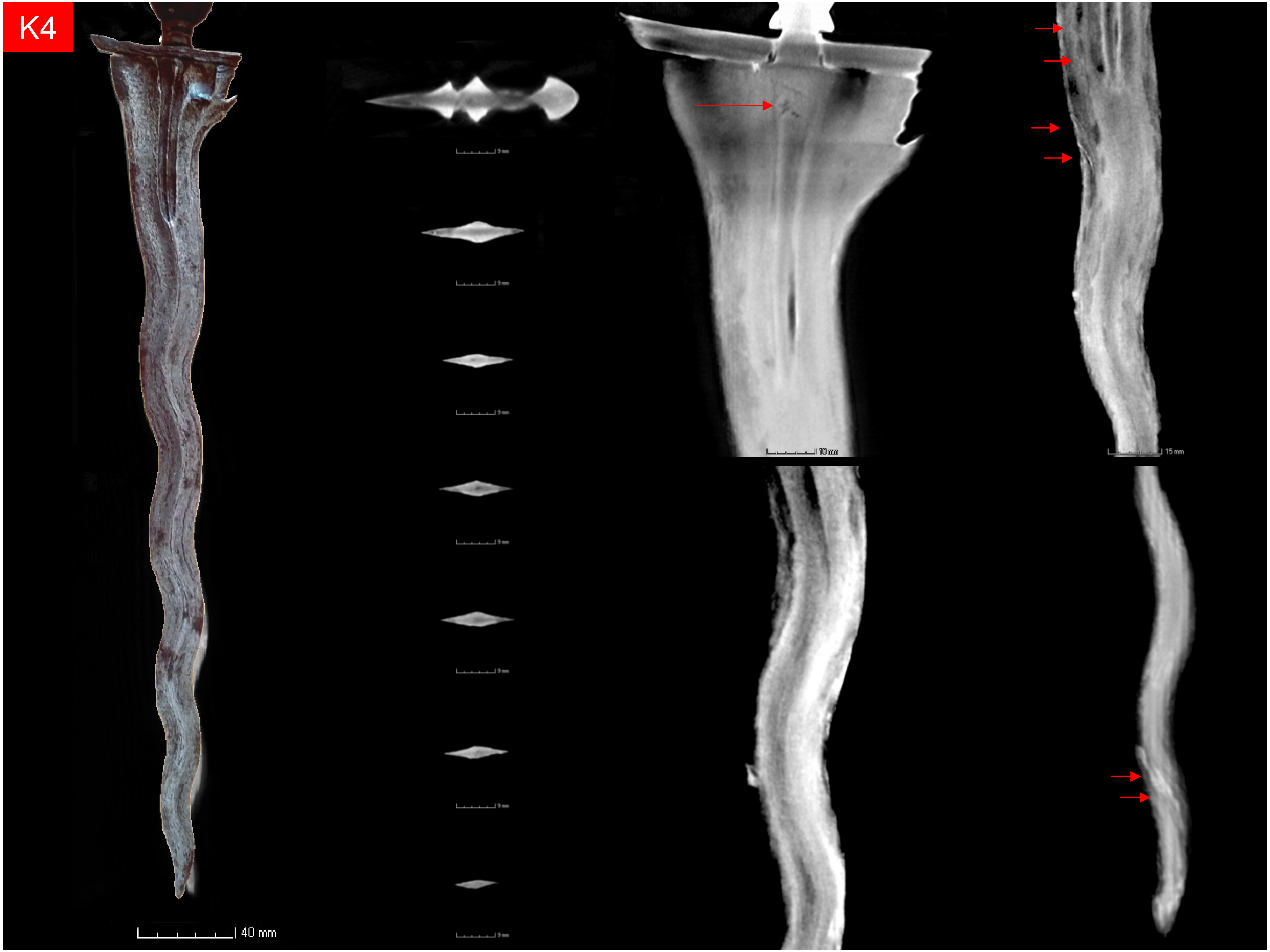
K4
40 mm
10 mm
15 mm

The Indian Wootz steel

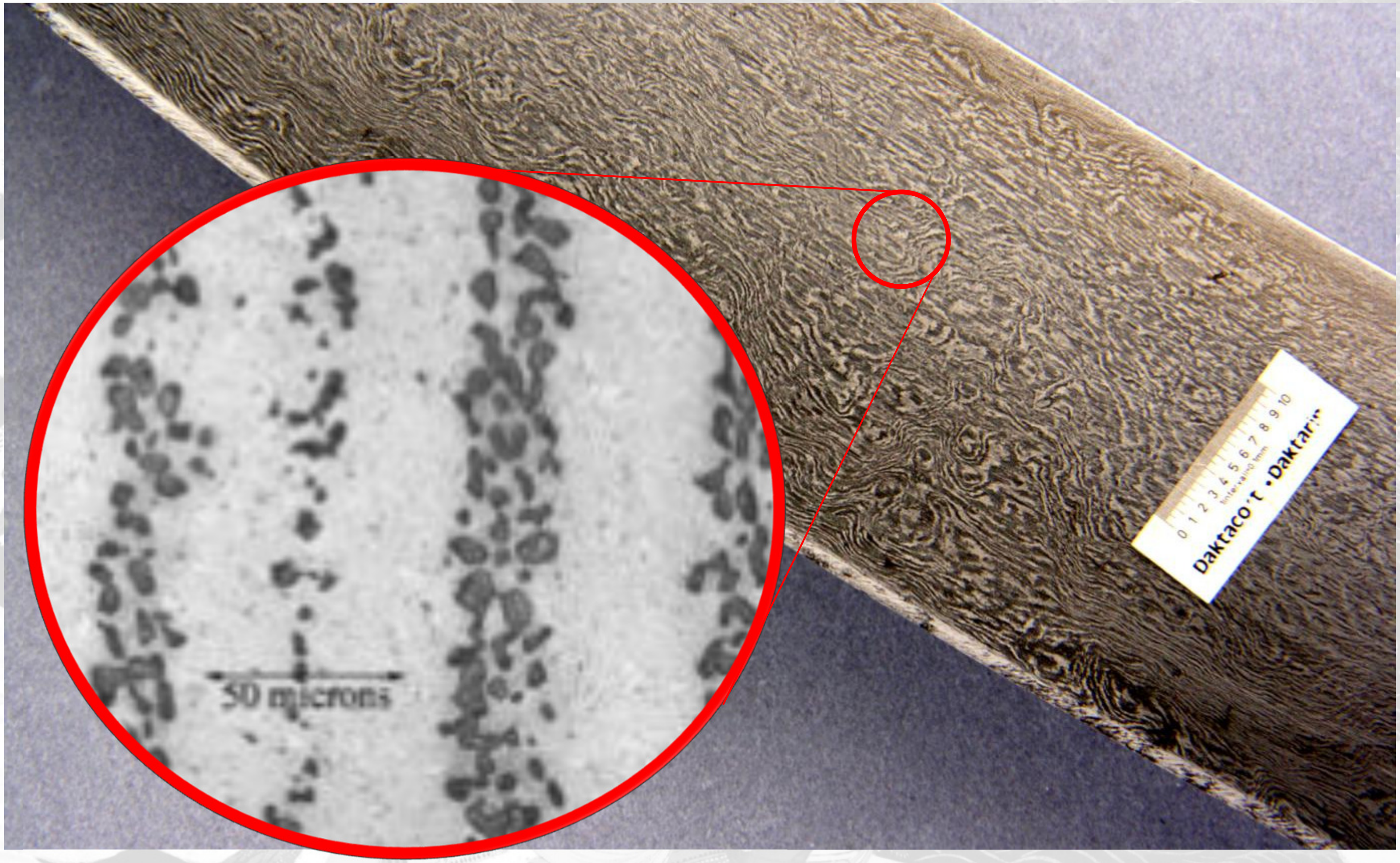

Hard and resilient homogeneous steel: no need of quenching, reshaping or polishing never affects mechanical properties.

The samples for neutron investigation

#4 18th Century blades exhibiting surface wootz like pattern

Energy-selective Tomography: Set-up optimization

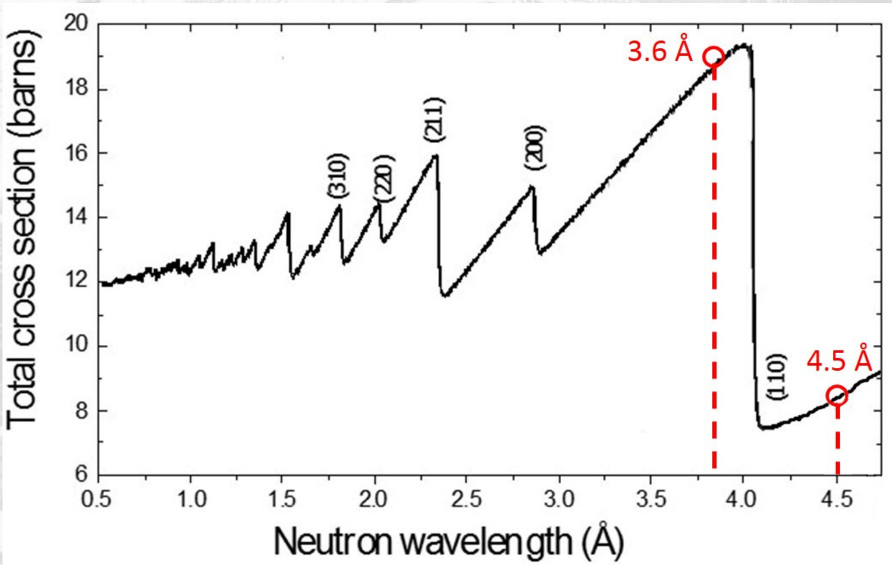

THE WALLACE COLLECTION

FRM II
Forschungs-Neutronenquelle
Heinz Maier-Leibnitz

Sword 8: Energy-selective neutron tomography

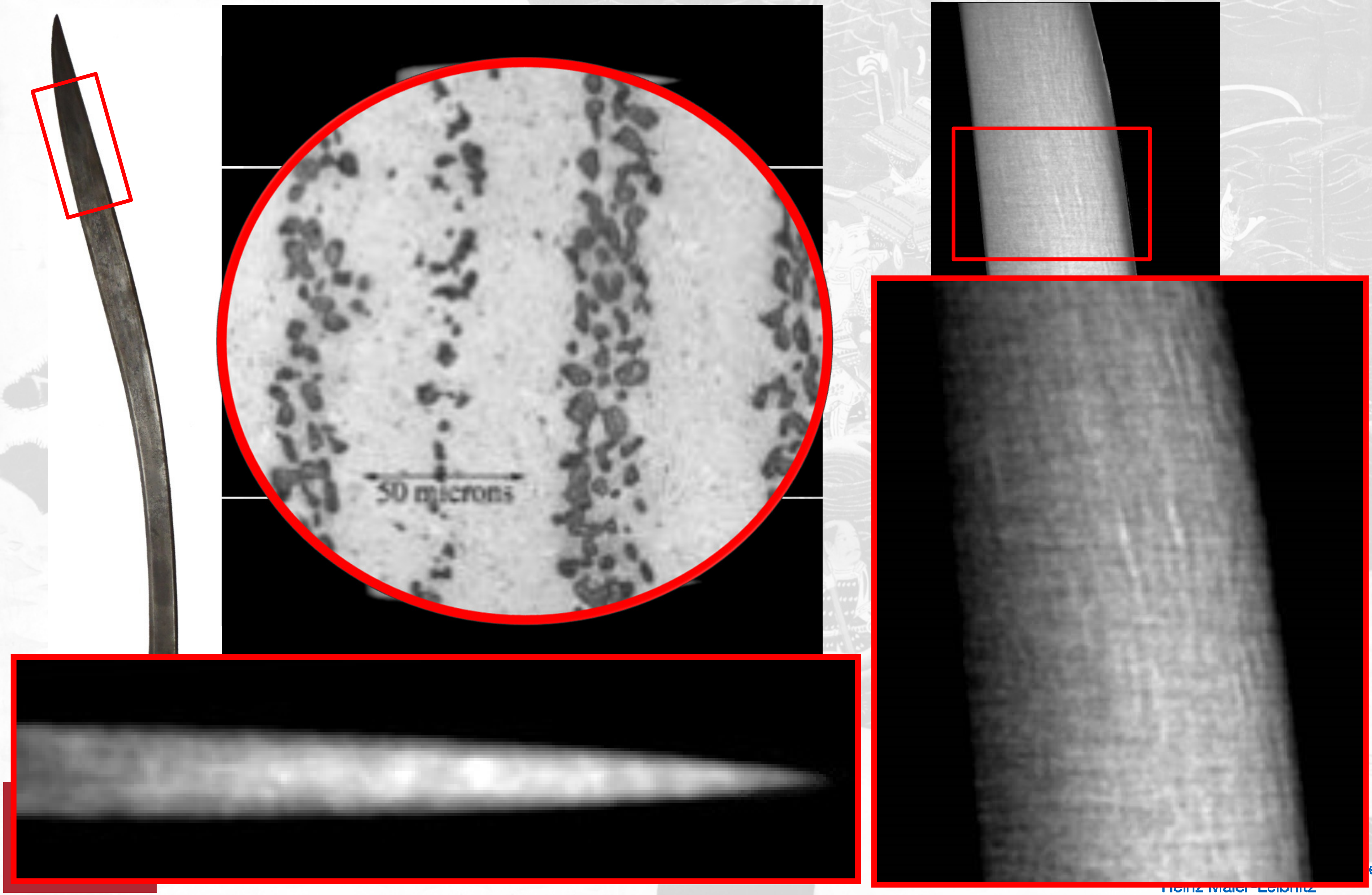

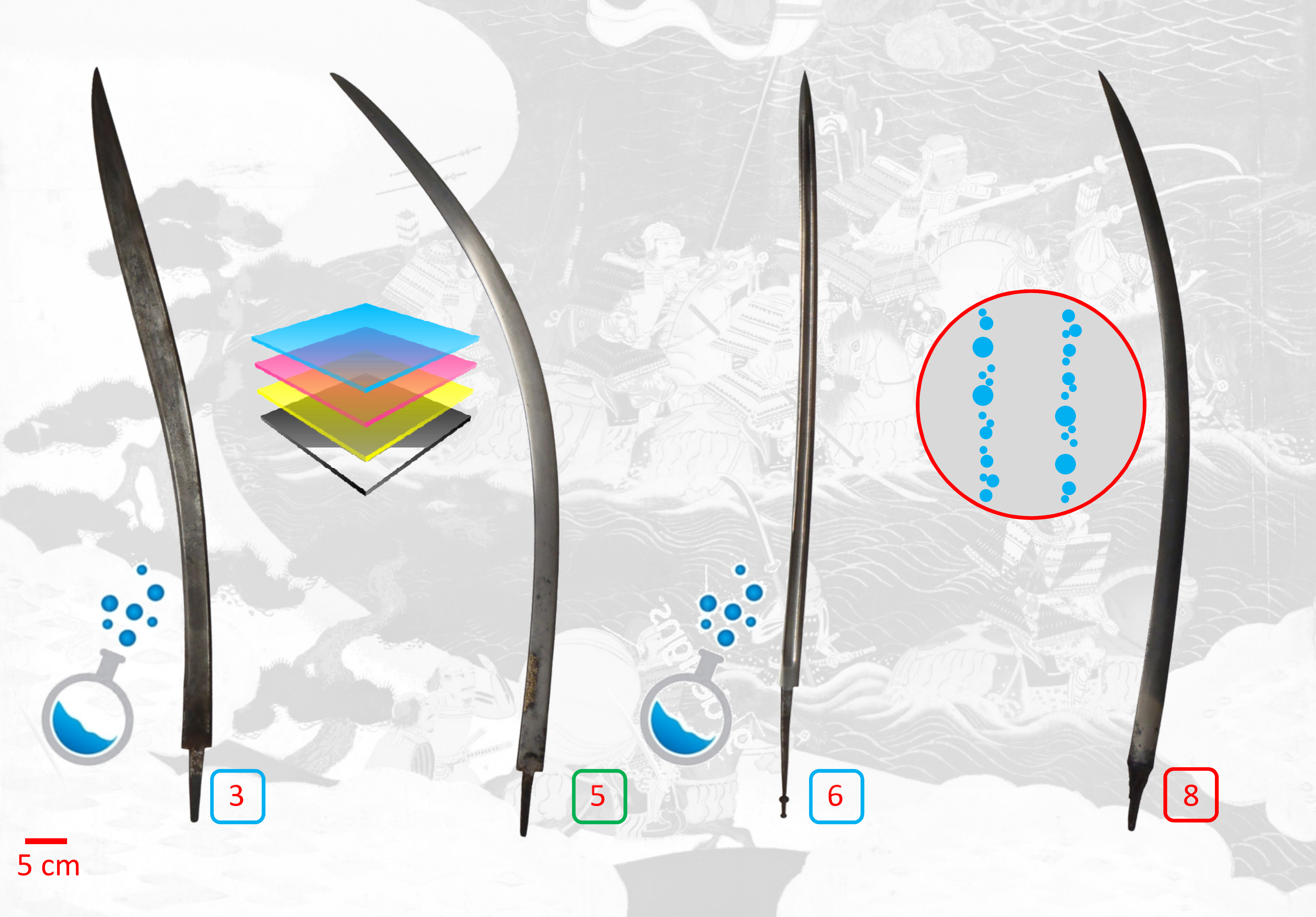
3
5
6
8
5 cm

Japanese sword: structure and making

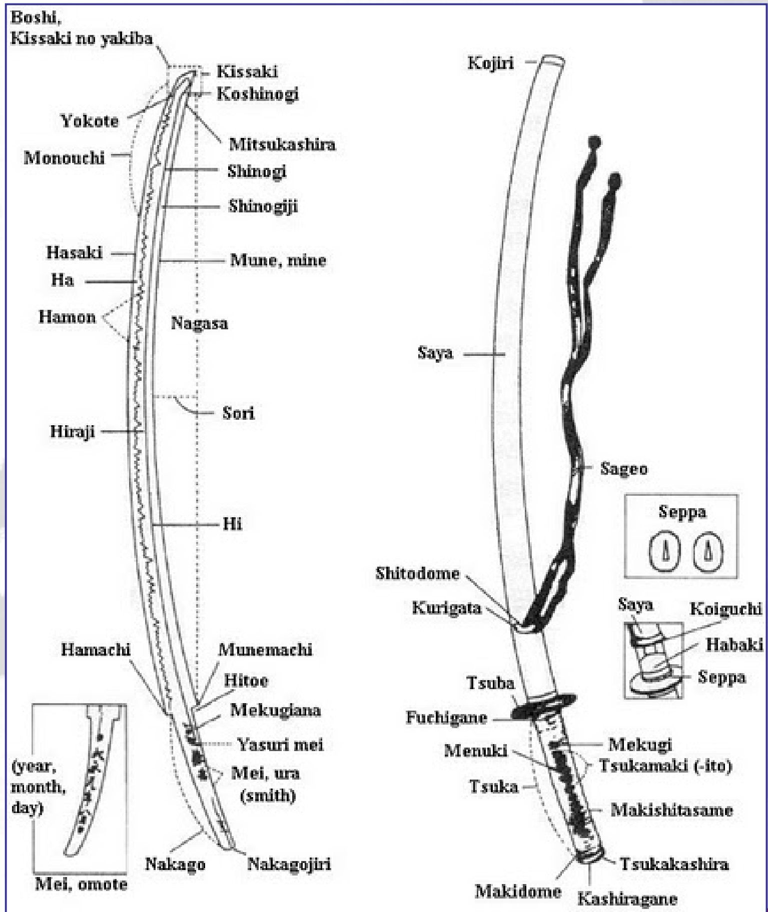

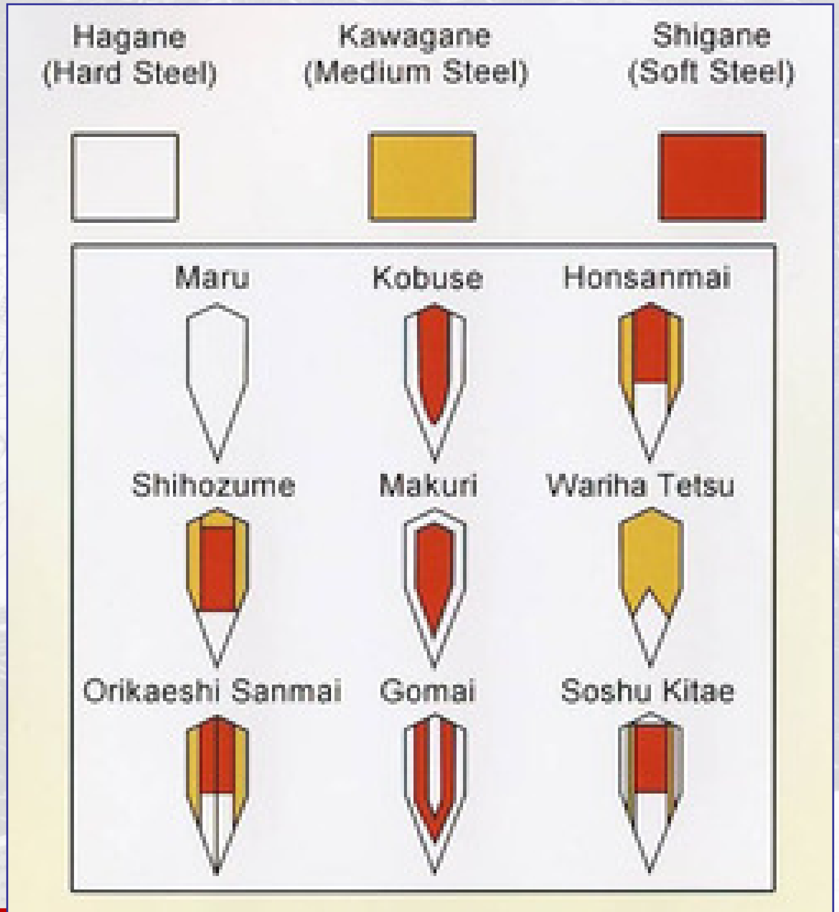

Single edge curved blade
Multiple hammering and folding steel
Composite structure
Differentially quenched and tempered